Zuse Institute Berlin

Takustr. 7
14195 Berlin
Germany

KAI HOPPMANN-BAUM[1], FELIX HENNINGS[2], JANINA ZITTEL[3], UWE GOTZES, EVA-MARIA SPRECKELSEN, KLAUS SPRECKELSEN, THORSTEN KOCH[4]

From Natural Gas towards Hydrogen – A Feasibility Study on Current Transport Network Infrastructure and its Technical Control

[1] 0000-0001-9184-8215
[2] 0000-0001-6742-1983
[3] 0000-0002-0731-0314
[4] 0000-0002-1967-0077

ZIB Report 20-27 (November 2020)

Zuse Institute Berlin
Takustr. 7
14195 Berlin
Germany

Telephone: +49 30-84185-0
Telefax: +49 30-84185-125

E-mail: bibliothek@zib.de
URL: http://www.zib.de

ZIB-Report (Print) ISSN 1438-0064
ZIB-Report (Internet) ISSN 2192-7782

From Natural Gas towards Hydrogen
—
A Feasibility Study on Current Transport Network Infrastructure and its Technical Control

Kai Hoppmann-Baum[1,2][0000−0001−9184−8215], Felix Hennings[1][0000−0001−6742−1983], Janina Zittel[2][0000−0002−0731−0314], Uwe Gotzes[3], Eva-Maria Spreckelsen[3], Klaus Spreckelsen[3], and Thorsten Koch[1,2][0000−0002−1967−0077]

[1] Technische Universität Berlin, Straße des 17. Juni 135, 10623 Berlin, Germany
{hoppmann,hennings,koch}@tu-berlin.de
[2] Zuse Institute Berlin, Takustr. 7, 14195 Berlin, Germany
{hoppmann-baum,zittel,koch}@zib.de
[3] Open Grid Europe GmbH, Kallenbergstr. 5, 45141 Essen, Germany
{uwe.gotzes,eva-maria.spreckelsen,klaus.spreckelsen}@oge.net

Abstract. This study examines the usability of a real-world, large-scale natural gas transport infrastructure for hydrogen transport. We investigate whether a converted network can transport the amounts of hydrogen necessary to satisfy current energy demands. After introducing an optimization model for the robust transient control of hydrogen networks, we conduct computational experiments based on real-world demand scenarios. Using a representative network, we demonstrate that replacing each turbo compressor unit by four parallel hydrogen compressors, each of them comprising multiple serial compression stages, and imposing stricter rules regarding the balancing of in- and outflow suffices to realize transport in a majority of scenarios. However, due to the reduced linepack there is an increased need for technical and non-technical measures leading to a more dynamic network control. Furthermore, the amount of energy needed for compression increases by 364% on average.

Keywords: Hydrogen Transport · Hydrogen Infrastructure · Network Flows · Mixed Integer Programming · Energiewende

1 Introduction

The envisaged global transition away from fossil fuels towards a CO_2-neutral energy supply confronts energy system planners and operators with new and complex challenges. The German Energiewende is a concrete realization of this process. Here, it becomes evident that any strategy based on renewable energy sources, which exclusively relies on electrical power, is not realizable, especially when considering industries depending on high thermal energy, such as steel

production [ORG+17], or the transport sector [Die20]. In addition, with an increasing share of renewable energy sources, it is a crucial task to design and build a sufficient storage and transport system. Thus, chemical energy carriers are needed and hydrogen-based technologies are a promising choice, which is underlined by the recently published national hydrogen strategy of the German government [Die20]. A multitude of technologies, e.g., green, turquoise, and blue hydrogen and variants of the Power-to-X conversion are possible options when implementing an infrastructure to produce, transport, and store energy.

In this context, the usage of pipeline networks and their connected storage facilities seems to be the most suitable approach [RGRS19,YO07]. However, planning and building new pipeline infrastructures is an expensive task, which has been investigated for natural gas [BS79,DG16,Hum17,RFR+70] and more recently for hydrogen and coupled systems [AAB+13,BGG+13,SSS16,WP18], too. Thus, the obvious looking idea of converting the existing billion Euro valued natural gas transport infrastructure into a hydrogen network is becoming more and more popular [Die20,DD13,Ada20]. The cost of a transformation is expected to be about 10-15% of the cost of a completely new construction, whose implementation process would additionally take at five to seven years from initial planning to commissioning in the best-case scenario [Ada20].

Besides the economic considerations, existing studies have mainly focused on the feasibility w.r.t. the technical components, e.g., whether the installed pipelines are actually suited for hydrogen transport or not [DD13,Ada20]. However, the question if and how the control of the network changes compared to the transport of natural gas is equally important and has been raised [DD13] but not yet been thoroughly investigated. It arises due to the different physical properties of the gases: For example, the linepack-energy capacity of a hydrogen converted network, i.e., the amount of energy that can be stored in the pipelines, might be just a quarter compared to natural gas [HD07a]. Furthermore, the operation of commonly used turbo compressors depends on the gas volume and the volumetric flow rate. Thus, either the rotational velocity would have to be increased, potentially raising material integrity concerns, or a higher number of serial compression stages would be required when transporting hydrogen [DD13,HD07a].

In this paper we examine whether a representative real-world pipeline network, which is currently used to transport natural gas, provides the capacity to transport the amounts of hydrogen that are necessary to satisfy current energy demands. Besides the feasibility of the idea in general, we are particularly interested in how the technical control of the network changes.

2 Related Work

As mentioned above, there have been several publications regarding the planning and building of natural gas pipeline networks. Bhaskaran and Salzborn [BS79] present an approach for determining a cost-optimal pipeline network from scratch, i.e., they determine junction points, pipes, and the corresponding diameters. In contrast, Rothfarb et al. [RFR+70] and Humpola [Hum17] discuss the expan-

sion of already existing infrastructures. Drouven and Großmann [DG16] propose a large-scale, nonconvex, mixed-integer nonlinear programming formulation to determine the most profitable shale gas development strategies. Their model involves planning, design, and strategic decisions such as where, when, and how many shale gas wells to drill and where to lay out the connecting pipelines.

For hydrogen, Andre et al. [AAB+13] introduce a nonlinear programming approach to determine a cost-minimal layout including the dimensioning of the pipes. They introduce a local search method and compare it with the results of a Tabu search heuristic. For the same problem, Weber and Papageorgiou [WP18] introduce an approximating mixed integer linear programming (MILP) formulation. Baufume et al. [BGG+13] present a transport system for Germany supplying the transport sector and demonstrate its economic feasibility. Further, Samsatli et al. [SSS16] design a wind-hydrogen-electricity network for domestic transport in Great Britain, which includes compressors, underground storages, and hydrogen transport pipelines.

Due to the inherent computational complexity of network design problems, many of the solution approaches only apply very simple models for the physics and the control of gas transport networks. In many cases only passive networks consisting only of pipelines or no temporal resolution are considered. Accordingly, most publicly available energy system optimization models do not take physical phenomena such as pressure drop into account, see Groissböck [Gro19]. But as Reuß et al. demonstrate [RWT+19], using different linear and nonlinear modelling approaches and applying certain network simplifications can have a huge impact when determining a cost-optimal layout.

Regarding more detailed modelling approaches for gas transport, the stationary case of determining a feasible network state given predefined boundary values, has gained a lot of attention during the last years. At this point, we refer to [KHPS15] for an extensive overview.

Only recently the transient case was subject to several publications. The first article to mention here is by [Mor07]. In this work, a mixed integer linear program (MILP) formulation where single compressor units are modelled separately is presented. Furthermore, the physics of gas flow through cyclindric pipelines are approximated using piecewise linear functions. In [MVHZ+16] and [ZCB15] pure nonlinear programming models (NLPs) are considered. Here, the task is to decide on compression ratios for the compressors, while the goal is to minimize their fuel consumption. In the work of [GLM+18] and [BEG+19], special discretization schemes for the Euler equations, a set of nonlinear hyperbolic partial differential equations describing the transient gas flow in cylindric pipelines, are applied and single compressor units are again modelled independently of each other. [BEG+19] impose lower and upper bounds on the compression ratios as well as on the achievable pressure differences of the compressor units. Their goal is to maximize the amount of gas stored in the network, i.e., the linepack. Therefore, a MILP and an NLP formulation are solved in an alternating fashion. In contrast, in [GLM+18] the deviation from future flow and pressure values is minimized by iteratively solving a MILP and an NLP model for each time step. Here, linear

feasible regions for the compressors are assumed. Next, the work in [HHLK19] and [HAH+19] combined can be seen as a two-stage approach. Here, the tri-level model in [HHLK19] determines global control decisions, such as flow directions and where to compress the gas in the network. Besides minimizing the usage of technical measures, its main goal is to minimize deviations from future flow and pressure values, too. Here, single compressor units are considered in a simplified configuration model. In [HAH+19] on the other hand, compressor stations are modelled in great detail. Here, the goal is to minimize the necessary changes in operation modes and related elements over time, while satisfying given flow and pressure time series.

In 2013, Dodds and Demoullin [DD13] discussed a complete transformation of the United Kingdom's natural gas network based on expert interviews and an extensive literature review. They find that whether existing pipes are suited for the transport of hydrogen depends on a number of factors including the material, the operating pressure, the age and the overall condition [HD07b]. The main concern at ambient temperature and pressures below 100 bar for high-strength steel is hydrogen embrittlement. However, they conclude that hydrogen can be transported safely when soft steel pipelines are used. Additionally, they recognize that the overall capacity of the system is reduced and that the storage capabilities due to linepack are much lower compared to natural gas. Finally, they do raise the question if and how the control of the network changes compared to the transport of natural gas. However, to the best of our knowledge it has not been investigated yet.

The contribution of this manuscript is threefold. First, we propose an optimization model for transient transport of hydrogen through pipeline networks. It includes modelling approaches for the compression of hydrogen by turbo and hydrogen compressors as well as for the transient flow of hydrogen through cyclindric pipelines. Additionally, since to the best of our knowledge no real-world instances for large-scale hydrogen pipeline networks exist, we introduce a methodology for the conversion of natural gas transport scenarios. Second, using this model we carry out a study to validate whether an existing natural gas pipeline network is suitable to transport the amounts of hydrogen necessary to satisfy current energy demands. And third, we demonstrate that the control of the network becomes more dynamic in the sense that there is an increased need for technical and non-technical control measures. Further, we show that the necessary compression energy increases by 364% on average.

3 Robust Control of Transient Hydrogen Networks

In this section, we introduce an algorithmic approach for the optimal robust control of transient hydrogen pipeline transport networks. It is an adaption and extension of the algorithm of Hoppmann et al. [HHLK19], which was originally designed for the transport of natural gas.

The approach features a mixed integer linear programming (MILP) formulation for the technical control of the network, which is embedded into the lowest

level of a tri-level model. The upper two levels represent a hierarchy of non-technical control measures and are incorporated as slack variables imposed on supplies and demands as well as on inflow pressure bounds. Due to the chosen design, these variables can only be nonzero if there exists no feasible control using technical components of the network. Subsequently, a sequential linear programming inspired post-processing routine is applied in order to derive physically more accurate solutions w.r.t. the transient gas flow in pipelines.

In the following, we give an overview of the approach and discuss those parts in depth, which differ between natural gas and hydrogen. In particular, we take a detailed look on the modelling of transient hydrogen flow through pipelines and discuss its compression in detail. For more information on all other topics, we refer to [HHLK19].

3.1 Basic Formulation

A pipeline transport network is modelled as a directed graph $G = (\mathcal{V}, \mathcal{A})$, where $\mathcal{V}$ denotes the set of nodes and $\mathcal{A}$ the set of arcs. Note that we allow parallel and anti-parallel arcs. Additionally, we consider time as a discrete and finite set of time steps $\mathcal{T}_0 := \{0, \dots, k\}$ together with a monotonically increasing function $\tau : \mathcal{T}_0 \to \mathbb{N}$, where $\tau(t)$ represents the number of seconds that have passed since $t = 0$. For notational purposes, let $\mathcal{T} := \mathcal{T}_0 \setminus \{0\}$.

The most important physical entity regarding the network nodes is pressure. For each $v \in \mathcal{V}$ we are given a non-negative initial pressure value $p_{v,0} \in \mathbb{R}_{\geq 0}$ and for each $t \in \mathcal{T}$ we introduce a pressure variable $p_{v,t} \in [\underline{p}_{v,t}, \bar{p}_{v,t}] \subseteq \mathbb{R}_{\geq 0}$. The lower and upper bounds $\underline{p}_{v,t}, \bar{p}_{v,t} \in \mathbb{R}_{\geq 0}$ are called technical pressure bounds.

Further, for each source $v \in \mathcal{V}^+ \subseteq \mathcal{V}$ we are given supply values $D_{v,t} \in \mathbb{R}_{\geq 0}$ and for each sink $v \in \mathcal{V}^- \subseteq \mathcal{V}$ we are given demand values $D_{v,t} \in \mathbb{R}_{\leq 0}$ for each $t \in \mathcal{T}$. Additionally, there exist additional lower and upper pressure bounds $\underline{p}^{\text{act}}_{v,t} \in \mathbb{R}_{\geq 0}$ and $\bar{p}^{\text{act}}_{v,t} \in \mathbb{R}_{\geq 0}$ for the sources and sinks, called inflow pressure bounds, which are tighter than the technical ones, i.e., $[\underline{p}^{\text{act}}_{v,t}, \bar{p}^{\text{act}}_{v,t}] \subseteq [\underline{p}_{v,t}, \bar{p}_{v,t}]$, and have to be respected in case that the corresponding node has nonzero supply or demand, respectively.

However, both, the demand and supply values as well as the inflow pressure bounds, can be dynamically adjusted if no feasible network control using technical measures only exists. This gives rise to a tri-level formulation, see Subsection 3.4 for more information. Hence, corresponding slack variables and constraints regarding these two entities are added to the model. For the supplies and demands, the actual values considered in the model are established through additional variables $d_{v,t} \in \mathbb{R}_{\geq 0}$ for each source $v \in \mathcal{V}^+$ and $d_{v,t} \in \mathbb{R}_{\leq 0}$ for each sink $v \in \mathcal{V}^-$ and constraints

$$d_{v,t} + \sigma^{d+}_{v,t} - \sigma^{d-}_{v,t} = D_{v,t} \quad \forall v \in \mathcal{V}^+ \cup \mathcal{V}^-, \forall t \in \mathcal{T}, \tag{1}$$

where $\sigma^{d+}_{v,t}, \sigma^{d-}_{v,t} \in \mathbb{R}_{\geq 0}$ are the so-called boundary value slack variables. Furthermore, for the inflow pressure bounds we introduce two continuous variables

$\sigma^{p+}_{v,t} \in [0, \underline{p}^{\text{act}}_{v,t} - \underline{p}_{v,t}]$ and $\sigma^{p-}_{v,t} \in [0, \bar{p}_{v,t} - \bar{p}^{\text{act}}_{v,t}]$ as well as constraints

$$p_{v,t} + \sigma^{p-}_{v,t} \geq \underline{p}^{\text{act}}_{v,t} \quad \forall v \in \mathcal{V}^+ \cup \mathcal{V}^- \text{ with } D_{v,t} \neq 0, \forall t \in \mathcal{T} \tag{2}$$

$$p_{v,t} - \sigma^{p+}_{v,t} \leq \bar{p}^{\text{act}}_{v,t} \quad \forall v \in \mathcal{V}^+ \cup \mathcal{V}^- \text{ with } D_{v,t} \neq 0, \forall t \in \mathcal{T}. \tag{3}$$

Here, $\sigma^{p+}_{v,t}$ and $\sigma^{p-}_{v,t}$ are called inflow pressure slack variables.

The most important physical entity regarding network arcs is mass flow. Although there are several different kinds of arcs in the network, each of them features for each point in time $t \in \mathcal{T}$ one or two variables corresponding to it, i.e., there are q-variables indexed with $t \in \mathcal{T}$ which either represent the current mass flow on an arc or, as it is the case for pipelines $\mathcal{A}^{\text{pi}} \subseteq \mathcal{A}$, which are explained in depth in Subsection 3.2, into and out of it. Finally, for each time step and each node we add flow conservation constraints, see [HHLK19] for more details.

Before we continue with detailed descriptions of the models for the different arc types, we conceptually divide the transport network into two parts. First, there are $m \in \mathbb{N}$ subgraphs $G_i = (\mathcal{V}_i, \mathcal{A}^{\text{ar}}_i)$ in G, which are called network stations and are mainly located at major pipeline crossings in the network. Each active element, i.e., each element that can be used to control the gas flow, is contained in one of these network stations. Second, the remaining network, called connecting network, which consists of pipelines only and connects network stations, entries, and exits with each other. Note that in contrast to [HHLK19] we do not consider valves and control valves separately anymore, since they can be modelled individually as network stations.

3.2 Connecting Network - Transient Hydrogen Flow in Pipelines

Pipelines are central elements regarding the modelling of transient gas transport networks. The following explanations are adapted from [HHLK19]. One-dimensional gas flow through cylindric pipelines is usually described by the so-called Euler equations, a set of nonlinear hyperbolic partial differential equations [Osi96]. As we assume isothermality in the following, i.e., the gas temperature remains constant over time, this set consists of the *Continuity Equation* and the *Momentum Equation*. While the first equation ensures the conservation of mass, the second describes the interaction between the force acting on the gas particles and the rate of change in their momentum. Let $a = (\ell, r) \in \mathcal{A}^{\text{pi}}$ be a pipeline. The isothermal Euler Equations can be stated as

$$\frac{\partial \rho}{\partial t} + \frac{\partial (\rho v)}{\partial x} = 0$$

$$\frac{\partial (\rho v)}{\partial t} + \frac{\partial p}{\partial x} + \frac{\partial (\rho v^2)}{\partial x} + \frac{\lambda_a}{2D_a} |v| v \rho + g s_a \rho = 0.$$

The p-variable denotes the pressure, while x represents the position in the pipe w.r.t. the distance from node ℓ. Furthermore, t denotes the time, and ρ and v the density and the velocity of the gas, respectively. Additionally, D_a denotes the diameter of the pipe and the gravitational acceleration is given by g. Further, by

λ_a we denote the friction factor of the pipe, which we derive from the formula of Nikuradse, see [FGG+15,Nik50]. This formula depends only on two characteristics of the pipe, namely its diameter and its integral roughness. Finally, the pipe's slope is given as $s_a = \frac{h_r - h_\ell}{L_a} \in [-1, 1]$, where h_ℓ and h_r denote the altitude at ℓ and r, respectively.

Since we are interested in mass flow q, pressure p, and velocity v we reformulate the equations accordingly. Thereby, mass flow is defined as

$$q = A_a \rho v, \tag{4}$$

where $A_a = D_a^2 \frac{\pi}{4}$ denotes the cross-sectional area of the pipe. Additionally, we apply the *equation of state for real gases*, which describes the relation between the gas pressure p and the density ρ

$$p = \rho R_s T z_a.$$

Here, T is the gas temperature, z_a is the compressibility factor of the gas in the pipe, and R_s denotes the specific gas constant. In the following, as for the temperature, we assume that the other two entities are constants, too. For the compressibility factor this is a common assumption, see for example [Osi96], and we define it as the average of the compressibility factors at both endnodes.

In contrast to the natural gas transport model [HHLK19], where the approximation formula of Papay is used, we apply a linear function, which is the result of a linear regression for a set of empirically measured values provided by OGE. Thus, for a pipe $a = (l, r) \in \mathcal{A}^{\mathrm{pi}}$ we define

$$z_a := \frac{\alpha(p_{l,0} + p_{r,0})}{2} + \beta, \tag{5}$$

where $p_{l,0}$ and $p_{r,0}$ are the initial pressures, $\alpha = 6.35882 \cdot 10^{-4}$, and $\beta = 0.99911$.

For the specific gas constant, this is a consequence of the fact that we assume the molar mass of the gas to be constant. However, it is important to note that, since the molar mass of hydrogen is about $\frac{1}{16}$ the molar mass of natural gas, its specific gas constant R_s is about 16 times greater.

Finally, we drop the first and the third summand in the Momentum Equation, as their contribution under typical operating conditions in gas transport networks is negligible, see [BEG+19,Osi96]. Putting all this together, we rewrite the two equations and derive the so-called friction dominated model

$$\begin{aligned} \frac{\partial p}{\partial t} + \frac{R_s T z_a}{A_a} \frac{\partial q}{\partial x} &= 0 \\ \frac{\partial p}{\partial x} + \frac{\lambda_a R_s T z_a}{2 D_a A_a^2} \frac{|q|q}{p} + \frac{g s_a}{R_s T z_a} p &= 0. \end{aligned}$$

Next, we discretize the equations using an implicit box scheme, which was proposed in [DGK+11,KLB10]. Here, the length of the pipe L_a serves as spacial domain while we use the set of time steps $\mathcal{T}_0$ as time domain. Therefore, we use continuous mass flow variables $q_{\ell,a,t} \in \mathbb{R}$ and $q_{r,a,t} \in \mathbb{R}$, where the first describes

the flow into the pipe at node ℓ and the second the flow out of the pipe at node r. The discretized equations for two adjacent time steps $t-1$ and t, where $t \in \mathcal{T}$, can then be written as

$$\begin{aligned} &\frac{2R_sTz_a(\tau(t)-\tau(t-1))}{L_aA_a}\left(q_{r,a,t}-q_{\ell,a,t}\right) \\ &\qquad + p_{\ell,t} + p_{r,t} - p_{\ell,t-1} - p_{r,t-1} = 0 \qquad \text{(C)} \\ p_{r,t} - p_{\ell,t} + \frac{\lambda_a R_s T z_a L_a}{4 D_a A_a^2} &\left(\frac{|q_{\ell,a,t}|q_{\ell,a,t}}{p_{\ell,t}} + \frac{|q_{r,a,t}|q_{r,a,t}}{p_{r,t}}\right) \\ &\qquad + \frac{g s_a L_a}{2R_sTz_a}\left(p_{\ell,t}+p_{r,t}\right) = 0. \qquad \text{(M)} \end{aligned}$$

Finally, as in Hoppmann et al. [HHLK19], we apply the linear model proposed by Hennings [Hen18], where the absolute velocity in the Momentum Equation is fixed to the initial velocity at $t = 0$. By doing so, we derive two linear equations:

$$\begin{aligned} &\frac{2\,R_s\,(\tau(t)-\tau(t-1))\,T\,z_a}{L_a\,A_a}\left(q_{r,a,t}-q_{\ell,a,t}\right) \\ &\qquad + p_{\ell,t} - p_{\ell,t-1} + p_{r,t} - p_{r,t-1} \;= 0 \;\forall t \in \mathcal{T} \qquad (6) \\ p_{r,t} - p_{\ell,t} + \frac{\lambda_a\,L_a}{4\,A_a\,D_a} &\left(|v_{\ell,0}|\,q_{\ell,a,t} + |v_{r,0}|\,q_{r,a,t}\right) \\ &\qquad + \frac{g\,s_a\,L_a}{2\,R_s\,T\,z_a}\left(p_{\ell,t}+p_{r,t}\right) \;= 0 \;\forall t \in \mathcal{T}. \qquad (7) \end{aligned}$$

The obvious issue arising here is that if the velocity of the mass flow in- or decreases significantly over time, we might under- or overestimate the friction loss, respectively. However, to overcome this problem, a post-processing routine inspired by sequential linear programming is applied, which is discussed in Subsection 3.6.

3.3 Network Stations - Controlling the Flow of Hydrogen

For each time step $t \in \mathcal{T}_0 := \{0, \ldots, k\}$ there is a hierarchy of three types of control decisions, which have to be taken for each network station G_i. First, exactly one so-called flow direction $f \in \mathcal{F}_i$ has to be chosen for each G_i. Choosing a flow direction implies which nodes of the network station serve as entries and exits w.r.t. in- and outflow via corresponding constraints. Additionally, a flow direction may enforce some upper (tighter) pressure bounds on some of the exits and it can come with some further conditions, i.e., minimum in- or outflow requirements on certain subsets of its entries or exits. Second, given a flow direction, one must additionally choose exactly one supporting simple state $s \in \mathcal{S}_i$. Whether a simple state supports a flow direction or not is previously known. A simple state can be seen as a set of technical control settings for all arcs in a station. Thus, it comes with a set of mandatory arcs s^{on}, which must be active, i.e., must be used according to their modelling. Its inactive arcs s^{off} on the other hand cannot be used and can be considered as nonexistent or closed valves.

For all remaining arcs $a \in \mathcal{A}_i^{\text{ar}} \setminus (s^{\text{on}} \cup s^{\text{off}}) =: s^{\text{opt}}$, which we call optional arcs, we can independently choose whether they are active or not, which represents the third type of control decisions. All these decisions, whether a flow direction, simple state or station arc is active, are modelled using binary variables and corresponding constraints.

Furthermore, there are additional constraints and in particular binary variables which indicate whether there was a change into simple state $s \in \mathcal{S}_i$ in time step t, represented by $\delta_{s,t} \in \{0,1\}$, or if an optional arc $a \in s^{\text{opt}}$ has been turned on or off, represented by $\delta_{a,t}^{\text{on}}, \delta_{a,t}^{\text{off}} \in \{0,1\}$, respectively. These decision variables are, besides the already mentioned slack variables, the only ones associated with some cost, i.e., they feature non-negative objective coefficients $w^s, w^a \in \mathbb{R}_{\geq 0}$. Thus, the goal of the optimization model is to find a feasible network control, such that the control decisions in the stations w.r.t. simple states and the activity of optional arcs are as constant as possible over time.

Next, we are going to describe the different types of arcs that are contained in the network stations. The first type is the so-called shortcut $a = (\ell, r) \in \mathcal{A}^{\text{ar-sc}}$. If it is active at time $t \in \mathcal{T}$ the pressures at ℓ and r have to be equal and mass flow can go into both directions. If it is not active, the pressure values are decoupled, i.e., independent of each other, and there is no flow.

The second arc type, so-called regulating arcs $a = (\ell, r) \in \mathcal{A}^{\text{ar-rg}}$, can be used to decrease the pressure in the direction of flow. If it is active the pressure at ℓ has to be greater or equal than the pressure at r and there can be arbitrarily high mass flow in forward direction. Otherwise, the pressure values are decoupled and there is no mass flow.

The third and the fourth type are the compressor arcs $\mathcal{A}^{\text{ar-co}}$ and the combined arcs $\mathcal{A}^{\text{ar-cb}}$. The latter can either be used as a regulating arc, as described above, or as a compressor arc, which we discuss in the following. The decision which of the modes is used is modelled by additional binary variables and constraints. The so-called pressure increasing arcs $\mathcal{A}^{\text{ar-pr}} := \mathcal{A}^{\text{ar-co}} \cup \mathcal{A}^{\text{ar-cb}}$ are key elements when it comes to the control of a gas network. They are able to compress gas and thereby increase the pressure in forward direction, which makes up for the pressure loss due to friction in the pipes and height differences.

In our model, one can conceptually think of one (big) compressor machine being installed on each arc $a \in \mathcal{A}_i^{\text{ar-pr}}$ of a gas network station G_i. The maximum power it has available for compression $\tilde{\pi}_{a,t} \in \mathbb{R}_{\geq 0}$, the maximum amount of mass flow that can pass through it $\tilde{q}_{a,t} \in \mathbb{R}_{\geq 0}$, and its maximum compression ratio $\tilde{r}_{a,t} \in [1, \infty)$ are dynamically determined in each time step through an assignment of approximated real-world compressor units and a linear combination of the corresponding entities, see [HHLK19]. While the latter two values are directly used as bounds on the possible mass flow and the pressure increase (w.r.t. the initial pressure value), the maximum power has an impact on all three due to the *power equation*.

When gas is compressed by a compressor machine, the connection between pressure ratio, the amount of mass flow passing through, and the power necessary

to realize it is given by the nonlinear power equation

$$\tilde{\pi}_{a,t} \geq \pi_{a,t} = \frac{q_{a,t}}{\eta_{\text{ad}}} R_s T z_\ell \frac{\kappa}{\kappa - 1} \left[\left(\frac{p_{r,t}}{p_{\ell,t}} \right)^{\frac{\kappa-1}{\kappa}} - 1 \right],$$

where $\pi_{a,t} \in \mathbb{R}_{\geq 0}$ is the variable representing the necessary power when a mass flow of $q_{a,t}$ with initial pressure $p_{\ell,t}$ shall be compressed up to $p_{r,t}$. Here, η_{ad} is the adiabatic efficiency of the compression, which we assume to be constant for all existing compressor machines. For hydrogen we consider a fixed isentropic exponent of $\kappa = 1.5$ and we again use the formula presented in equation (5) for the compressibility factor at node ℓ. Afterwards, we apply the sampling procedure described in [HHLK19] to derive a linear approximation.

It is important to note, that the maximum compression ratios of turbo compressor units drop when hydrogen instead of natural gas is compressed [DD13]. In the following, we empirically quantify this. For the sake of simplicity, we identify natural gas with its main component methane and assume a reference temperature of $T = 25\,^\circ\text{C}$ and a reference pressure of $p = 50\,\text{bar}$. Note that we index hydrogen and methane related quantities with H_2 and CH_4 superscripts, respectively. The feasible operating range of a turbo compressor unit is typically described by a so-called characteristic diagram in the dimensions $(H_{\text{ad}}, \frac{p_r}{p_\ell})$, where H_{ad} is the change of adiabatic enthalpy defined as

$$H_{\text{ad}} = R_s T z_\ell \frac{\kappa}{\kappa - 1} \left[\left(\frac{p_r}{p_\ell} \right)^{\frac{\kappa-1}{\kappa}} - 1 \right].$$

Recall that the specific gas constant R_s is defined as the ideal gas constant divided by the molar mass. Thus, we have $\frac{R_s^{H_2}}{R_s^{CH_4}} \approx \frac{16}{2} = 8$. Furthermore, using Papay's [Pap68] formula for methane and the linear formula (5) for hydrogen, we derive compressibility factors of 0.91 and 1.03, respectively. Finally, for $\kappa^{H_2} = 1.5$ and $\kappa^{CH_4} \approx 1.3$ as isentropic exponents, we derive the following relation for the compression ratios $r = \frac{p_r}{p_\ell}$ for the same value of H_{ad}:

$$r^{H_2} \approx \left(1 + \frac{1}{6.27} \left[(r^{CH_4})^{\frac{3}{13}} - 1 \right] \right)^3.$$

For some example compression ratios of turbo compressors w.r.t. natural gas, we derive the following compression ratios for H_2

r^{CH_4}	1.00	1.20	1.40	1.60	1.80	2.00	2.20	2.40	2.60	2.80	3.00
r^{H_2}	1.00	1.02	1.04	1.06	1.07	1.09	1.10	1.11	1.12	1.13	1.14

which coincides with the following rule of thumb regarding the maximum compression ratio of a turbo compressor for hydrogen given the natural gas data

$$r^{H_2} \approx 1 + \frac{r^{CH_4} - 1}{10}. \tag{8}$$

3.4 Tri-Level Model and Objectives

The tri-level model can be stated as follows:

$$\begin{aligned}
&\min_{\sigma^p} \sum_{t\in\mathcal{T}} \sum_{v\in\mathcal{V}^{\mathrm{b}}} (\sigma^{p+}_{v,t} + \sigma^{p-}_{v,t}) \\
&\quad \min_{\sigma^d} \sum_{t\in\mathcal{T}} \sum_{v\in\mathcal{V}^{\mathrm{b}}} (\sigma^{d+}_{v,t} + \sigma^{d-}_{v,t}) \\
&\qquad \min_{\cdots} \sum_{t\in\mathcal{T}} \Big(\sum_{s\in\mathcal{S}} w^s \delta_{s,t} + \sum_{a\in\mathcal{A}^{\mathrm{ar}}} w^a (\delta^{\mathrm{on}}_{a,t} + \delta^{\mathrm{off}}_{a,t})\Big) \\
&\qquad\quad \text{s.t. } \textit{constraints...}
\end{aligned}$$

All model constraints mentioned or introduced above are contained in the third level of the tri-level mixed integer linear program, while the upper two levels do not feature any constraints. The goal of the third level is to minimize the sum of the switching cost w.r.t. simple states and artificial arcs. Thereby, it is in charge of all but the two classes of slack variables. The second level minimizes the sum of the slack variables corresponding to the supply and demand values, which it simultaneously is in charge of. And analogously, the goal of the first level is to minimize the sum of the slack variables corresponding to inflow pressure bounds, which it simultaneously is in charge of. Using this optimization model, supply and demand slack are only used if the original supplies and demands cannot be satisfied using technical control measures only, i.e., by switching simple states or optional arcs. Furthermore, the inflow pressure bounds can only be relaxed if no feasible control exists even when supply and demand values are changed. For more details and the algorithm to solve this model, we refer to [HHLK19].

3.5 Solution Smoothening

Due to the nature of LP-based branch-and-bound algorithms, such as the one provided by *Gurobi* [GO20], which we use for our computational experiments in Section 4, a typical issue that arises is the nonsmoothness of solutions. This can for example be observed on compressing arcs, where in many cases massive amounts of gas are compressed in a single time step, while there is basically no compression at all in all other time steps. Instead, we would like to have a steady mass flow over the whole time horizon, if possible. Similarly, the same behaviour can be observed for the outgoing pressures. Of course, these solutions with big differences in the corresponding variable values for consecutive time steps may be feasible w.r.t. the model, but such a behaviour is not desirable in practice.

Thus, given a solution for the tri-level formulation, we fix all binary values, add additional continuous variables and constraints, and solve the resulting linear program (LP) in order to determine a solution minimizing the changes in the inflow and pressure values at the boundary nodes of network stations for consecutive time steps, see [HHLK19].

3.6 Iterative Velocity Adjustment Procedure

A main drawback of the linear model for the transient gas flow through pipelines used in our MILP formulation is the fixation of the absolute velocity in the friction term of the Momentum Equation to the velocity at $t = 0$, see (7) in Subsection 3.2. If the mass flows or pressures at the endnodes of a pipeline change significantly for future time steps, we under- or overestimate the pressure loss, what in turn may lead to inaccurate decisions. Thus, we introduce an iterative velocity adjustment procedure (IVAP) here, which is an updated version of the routine proposed in [HHLK19]. However, its goal remains the same: To derive solutions, which are feasible for the tri-level MILP featuring nonlinear constraints (M) instead of (7).

The main idea is the following: Given a solution S for the tri-level model, we consider the linear program derived by fixing all binary variables to the corresponding solution values and using the gas velocities at the endnodes of all pipelines w.r.t. to S in the friction terms of the linear model for the Momentum Equations. The goal of the LP shall be to determine a solution such that the pressure and flow variables in constraints (7) stay as close as possible to the corresponding solution values in S. In case that there exists a solution such that all these variable values are equal, we have determined a solution satisfying constraints (M), as the gas velocity depends only on the mass flow and the pressure in our model, see (4). Thus, we introduce additional variables and constraints to measure deviations and penalize them in the LP's objective function. Therefore, we denote the set of vertices incident to a pipeline by $\mathcal{V}^{\text{pi}} := \bigcup_{(\ell,r)\in\mathcal{A}^{\text{pi}}}\{\ell, r\}$ and denote by ${}^{S}p_{v,t}$ ${}^{S}q_{a,\ell,t}$, and ${}^{S}q_{a,r,t}$ the solution values of the corresponding variables.

First, we add variables $\delta^{p+}_{v,t}, \delta^{p-}_{v,t} \in \mathbb{R}_{\geq 0}$ for each node $v \in \mathcal{V}^{\text{pi}}$ and each time step $t \in \mathcal{T}$. Furthermore, we add one additional variable $\overline{\delta}^{p}$ and constraints

$$p_{v,t} - {}^{S}p_{v,t} = \delta^{p+}_{v,t} - \delta^{p-}_{v,t} \qquad \forall v \in \mathcal{V}^{\text{pi}},\, \forall t \in \mathcal{T} \tag{9}$$

$$\delta^{p+}_{v,t} + \delta^{p-}_{v,t} \leq \overline{\delta}^{p} \qquad \forall v \in \mathcal{V}^{\text{pi}},\, \forall t \in \mathcal{T}. \tag{10}$$

Constraint (9) measures the difference of the pressure value of node v and time step t to the corresponding solution value in S using variables $\delta^{p+}_{v,t}$ and $\delta^{p-}_{v,t}$. The maximum difference for any node and any time step is determined by constraint (10) and is equal to variable $\overline{\delta}^{p}$. While $\overline{\delta}^{p}$ has objective coefficient $\overline{w}^{\text{sm-p}} \in \mathbb{R}_{\geq 0}$, we have cost $w^{\text{sm-p}} \in \mathbb{R}_{\geq 0}$ for all variables $\delta^{p+}_{v,t}$ and $\delta^{p-}_{v,t}$.

Second, for each pipeline $a = (\ell, r) \in \mathcal{A}^{\text{pi}}$ and each time step $t \in \mathcal{T}$ we add four continuous variables $\delta^{q+}_{a,\ell,t}, \delta^{q-}_{a,\ell,t}, \delta^{q+}_{a,r,t}, \delta^{q-}_{a,r,t} \in \mathbb{R}_{\geq 0}$ as well as one additional variable $\overline{\delta}^{q} \in \mathbb{R}_{\geq 0}$ and introduce constraints

$$q_{a,\ell,t} - {}^{S}q_{a,\ell,t} = \delta^{q+}_{a,\ell,t} - \delta^{q-}_{a,\ell,t} \qquad \forall a = (\ell, r) \in \mathcal{A}^{\text{pi}},\, \forall t \in \mathcal{T} \tag{11}$$

$$q_{a,r,t} - {}^{S}q_{a,r,t} = \delta^{q+}_{a,r,t} - \delta^{q-}_{a,r,t} \qquad \forall a = (\ell, r) \in \mathcal{A}^{\text{pi}},\, \forall t \in \mathcal{T} \tag{12}$$

$$\delta^{q+}_{a,\ell,t} + \delta^{q-}_{a,\ell,t} \leq \overline{\delta}^{q} \qquad \forall a = (\ell, r) \in \mathcal{A}^{\text{pi}},\, \forall t \in \mathcal{T} \tag{13}$$

$$\delta^{q+}_{a,r,t} + \delta^{q-}_{a,r,t} \leq \overline{\delta}^{q} \qquad \forall a = (\ell, r) \in \mathcal{A}^{\text{pi}},\, \forall t \in \mathcal{T}. \tag{14}$$

Algorithm 1: Iterative Velocity Adjustment Procedure (IVAP)

Input : Solution S_0 for tri-level MILP model L, k, ε
Output: Solution for L with constraints (M) instead of (7) or `UNSUCCESSFUL`

$v_0 \leftarrow$ Gas velocities at all $v \in \mathcal{V}^{\mathrm{pi}}$ w.r.t. S_0
$i \leftarrow 1$
repeat
  $v_i^* \leftarrow \sum_{j=\max\{0,i-k\}}^{i-1} \frac{v_j}{\min\{i,k\}}$
  $\mathrm{LP}_{\mathrm{iv}}^i \leftarrow \mathrm{LP}_{\mathrm{base}}(S_{i-1})$ with $|v_i^*|$ used in (7) and $\mathrm{MG}(S_0)$
  Solve $\mathrm{LP}_{\mathrm{iv}}^i$
  if $LP_{iv}^i = \mathit{INFEASIBLE}$ **then**
    return `UNSUCCESSFUL`
  end
  $S_i \leftarrow$ Optimal solution for $\mathrm{LP}_{\mathrm{iv}}^i$
  $v_i \leftarrow$ Velocities at all $v \in \mathcal{V}^{\mathrm{pi}}$ w.r.t. S_i
  $i \leftarrow i + 1$
until $|||v_i| - |v_i^*|||_\infty \leq \varepsilon$
return S_i

Here, constraints (11) and (12) determine the difference between the in- or outflow at the endnodes ℓ and r of pipeline a and the corresponding solution values in S. The maximum difference for any pipe, endnode and time step is determined by constraints (13) and (14) and is equal to $\overline{\delta}^q$, since it has nonzero objective coefficient $\overline{w}^{\text{sm-q}} \in \mathbb{R}_{\geq 0}$. For the other four variables $\delta_{a,\ell,t}^{q+}, \delta_{a,\ell,t}^{q-}, \delta_{a,r,t}^{q+}, \delta_{a,r,t}^{q-} \in \mathbb{R}_{\geq 0}$ we have cost $w^{\text{sm-q}} \in \mathbb{R}_{\geq 0}$. All other variables are assigned zero as objective coefficient. The resulting LP we denote by $\mathrm{LP}_{\mathrm{base}}(S)$.

However, first experiments showed that in the proposed LP formulation many slack variables were nonzero or attained values of higher magnitudes in the LP solution compared to the input solution S. On the other hand, when fixing all slack variables to their solution values in S, LP formulations turned out to be infeasible. These observations gave rise to a middle ground: For both classes of slack variables we set an additional upper bound equal to $\gamma \in \mathbb{R}_{\geq 0}$ times the corresponding solution values, which we denote by ${}^S\sigma_{v,t}^{d+}$, ${}^S\sigma_{v,t}^{d-}$, ${}^S\sigma_{v,t}^{p\mp}$, and ${}^S\sigma_{v,t}^{p-}$, i.e., constraints

$$\sigma_{v,t}^{d+} \leq \gamma \cdot {}^S\sigma_{v,t}^{d+} \quad \forall v \in \mathcal{V}^{\mathrm{b}}, \forall t \in \mathcal{T} \tag{15}$$

$$\sigma_{v,t}^{d-} \leq \gamma \cdot {}^S\sigma_{v,t}^{d-} \quad \forall v \in \mathcal{V}^{\mathrm{b}}, \forall t \in \mathcal{T} \tag{16}$$

$$\sigma_{v,t}^{p+} \leq \gamma \cdot {}^S\sigma_{v,t}^{p+} \quad \forall v \in \mathcal{V}^{\mathrm{b}}, \forall t \in \mathcal{T} \tag{17}$$

$$\sigma_{v,t}^{p-} \leq \gamma \cdot {}^S\sigma_{v,t}^{p-} \quad \forall v \in \mathcal{V}^{\mathrm{b}}, \forall t \in \mathcal{T} \tag{18}$$

were added. Note that by doing so, slack variables with solution value zero are fixed and the solution values of the slack variables in an optimal LP solution stay within a controllable range w.r.t. the S solution. This set of constraints we denote by $\mathrm{MG}(S)$.

Algorithm 2: Algorithmic Framework

Input : Tri-level MILP formulation L_1, Δ,k, ε
Output: Solution for L_1 with Momentum Equations (M) or `UNSUCCESSFUL`

$i \leftarrow 1$
while $i \leq \Delta$ **do**
  $S_i \leftarrow$ Solve L_i
  if S_i = *INFEASIBLE* **then**
    return `UNSUCCESSFUL`
  end
  $S_i^{sm} \leftarrow$ Solution of $\mathrm{LP}_{sm}(S_i)$
  $S_i^{iv} \leftarrow \mathrm{IVAP}(S_i^{sm}, k, \varepsilon)$
  if $S_i^{iv} \neq$ *UNSUCCESSFUL* **then**
    return S_i^{iv}
  $v_i^{\text{update}} \leftarrow$ velocities from last IVAP iteration
  $L_{i+1} \leftarrow L_i$ with v_i^{update} used in Momentum Equations (7)
  Add no-good-cut w.r.t. values of simple state variables $x_{s,t}$ in S_i to L_{i+1}
  $i \leftarrow i + 1$
end
return `UNSUCCESSFUL`

The iterative velocity adjustment procedure (IVAP) can now be stated as shown in Algorithm 1: Given a feasible solution S_0 for the initial hierarchical MILP model L, we first of all determine the gas velocities for all $v \in \mathcal{V}^{\text{pi}}$ and all time steps w.r.t. S_0. Next, we iteratively repeat the following procedure: In iteration i, we are going to use the absolute value of the average gas velocities from the last $\min\{i, k\}$ solutions, i.e., $|v_i^*|$, in constraints (7). Thus, we obtain linear program $\mathrm{LP}_{\text{iv}}^i$ as $\mathrm{LP}_{\text{base}}(S_{i-1})$ using $|v_i^*|$ in constraints (7) together with constraints (9) - (14) and $\mathrm{MG}(S_0)$. If $\mathrm{LP}_{\text{iv}}^i$ is infeasible, the procedure is terminated and `UNSUCCESSFUL` is returned. Otherwise we retrieve the gas velocities v_i from an optimal solution S_i. If $|v_i|$ and $|v_i^*|$ differ by less than ε for all pipelines, nodes and time steps, S_i is returned as result.

3.7 Complete Algorithmic Approach

The complete algorithmic approach, which is stated as Algorithm 2, is iteratively repeating the following procedure: In iteration i, we solve the tri-level MILP formulation L_i. If the model is infeasible, `UNSUCCESSFUL` is returned. Otherwise, we apply the smoothing routine to its solution S_i and start the IVAP with the resulting S_i^{sm}. If the IVAP terminates with a feasible solution, its a feasible solution for L with constraints (M) instead of (7) and Algorithm 2 is terminated. Otherwise, we retrieve the velocities v_i^{update} from the last IVAP iteration and derive a new tri-level MILP formulation L where constraints (7) are updated using the corresponding absolute values in the friction terms. Further, we add a

$\lvert\mathcal{V}\rvert$	$\lvert\mathcal{V}^+\rvert$	$\lvert\mathcal{V}^-\rvert$	$\lvert\mathcal{A}^{\mathrm{pi}}\rvert$	$\lvert\mathcal{A}^{\mathrm{ar}}\rvert$
179	12	89	149	72

Table 1. Composition of the macroscopic gas network.

no-good-cut w.r.t. the simple state variable values in S_i to L, i.e.,

$$\sum_{s\in\mathcal{S}}\sum_{t\in\mathcal{T}_0} x_{s,t}^{S_i}\cdot\, x_{s,t} \leq m\cdot|\mathcal{T}_0|-1$$

where $x_{s,t}^{S_i}$ denotes the corresponding variable value in S_i, $|\mathcal{T}_0|$ is the number of time steps, and m the number of network stations. The algorithm terminates with `UNSUCCESSFUL` if no solution within Δ iterations is found.

4 Computational Experiments

In this section we present computational experiments to test whether a real-world natural gas transport network is suited for the transport of hydrogen. In particular, we want to analyze whether the transport of hydrogen in a converted network is possible and how the control of the network changes.

4.1 Test Sets

For our computational experiments, we created five test sets that build on the 333 instances from natural gas transport used in [HHLK19], which are based on a real-world network together with the corresponding past measured data. The overall composition of the network is the same for all five test sets and depicted in Table 1. Likewise, the properties of the seven main network stations are shown in Table 2. Additionally, we have five network stations modelling a single control valve. We considered a temporal granularity of $2\cdot 60$ minutes and $11\cdot 120$ minutes, i.e., we used $n=13$ time steps covering a time horizon of 24 hours. The parameters and weights for all instances and test sets are listed in the Appendix.

Name	$\lvert\mathcal{V}_i^{\mathrm{fn}}\rvert$	$\lvert\mathcal{V}_i^{\mathrm{ar}}\rvert$	$\lvert\mathcal{A}_i^{\mathrm{ar}}\rvert$	$\lvert\mathcal{A}_i^{\text{ar-pr}}\rvert$	$\lvert\mathcal{F}_i\rvert$	$\lvert\mathcal{S}_i\rvert$
A	2	0	3	2	3	5
B	2	0	4	3	2	5
C	6	1	10	1	4	4
D	3	0	5	3	6	10
E	6	0	9	2	12	13
F	6	2	12	3	3	14
G	10	2	24	5	18	32

Table 2. Overview of the properties of the 7 main network stations A to G.

The five test sets differ in terms of the gas to be transported, in the volumetric amount of in- and outflow and in the composition and type of the compressors.

In the first test set natural gas is transported, based on the original real-world instances presented in [HHLK19] using turbo compressors. This test set serves as a reference for the four hydrogen test sets and we denote it by `CH4`.

Next, we created four different test sets for hydrogen transport. However, preliminary experiments indicated that the installed turbo compressors, which only allow for a maximum compression ratio according to Equation (8) on Page 10, are not sufficient for hydrogen transport, since instances could only be solved using massive amounts of inflow and/or pressure slack. Therefore, for the hydrogen transport test sets, in a first step we replaced each turbo compressor with a hydrogen compressor, which maintains the maximum compression ratio by comprising multiple serial compression stages, the maximum power, and the maximum flow.

The instances in the second test set, called `H2`, are equivalent to the instances in `CH4` in terms of the initial state and the supplies and demands w.r.t. volumetric flow. However, here we apply the algorithmic approach described in Section 3, where several adaptions, primarily due to the different physical properties of the gases, have been made.

Due to the lower energy density of hydrogen the amount of energy transported by natural gas in test set `CH4` is about 3.13 times bigger as in the hydrogen test set `H2`, since we have

$$3.13 \approx \frac{39.831 \frac{MJ}{m^3}}{12.745 \frac{MJ}{m^3}} = \frac{H_{s,n}(CH_4)}{H_{s,n}(H_2)},$$

where $H_{s,n}(CH_4)$ and $H_{s,n}(H_2)$ denote the calorific values of methane, as approximation for natural gas, and hydrogen [C+92], respectively. Thus, to evaluate the feasibility of hydrogen transport w.r.t. the transported energy we need to increase the in- and outflows accordingly.

Obviously, it is not meaningful to directly fully scale up the in- and outflows starting from time step $t = 1$, since the network state at $t = 0$ does not reflect this load situation. Hence, we allow for some ramp-up time for the network in order to adapt to higher volumetric flow values. Given some scaling factor $\xi \geq 1$, we define

$$\tilde{D}_{v,t} := D_{v,t} + \frac{\min\{t, 8\}\,(\xi - 1)}{8} D_{v,t} \quad \forall v \in \mathcal{V}^+ \cup \mathcal{V}^-,\, \forall t \in \mathcal{T}.$$

Thus, in the first 7 time steps, i.e., the first 12 hours, the supplies and demands are slowly increased, while for last 12 hours they are fully scaled by ξ. Additionally, to allow for a more reasonable modelling w.r.t. the transient gas flow, we applied the same ramp up technique to the absolute velocity fixed in the friction term of the Momentum Equations (7), i.e., we defined

$$|v_{\ell,t}| := v^{used} + \frac{\min\{t, 8\}\,(\xi - 1)}{8} v^{used} \quad \forall \ell \in \mathcal{V}^{\mathrm{pi}},\, \forall t \in \mathcal{T}.$$

Here, v^{used} is the maximum of the absolute gas velocity in the initial time step at the corresponding node $|v_{\ell,t}|$ and $v^{min} := 0.1\frac{m}{s}$. The introduction of the threshold v^{min} is necessary in order to control the magnitudes of the constraint's coefficients and to thereby avoid numerical instabilities.

With this procedure, we created three more test sets with increasing energy flows varying ξ from $\xi = \frac{1}{2} \cdot 3.13$, which we call `H2-12`, $\xi = \frac{3}{4} \cdot 3.13$, which we call `H2-34`, and $\xi = 3.13$, which we call `H2-EQ`. Thus, we consider half, three-quarter, and the equivalent amount of energy compared to natural gas in these three test sets, respectively. Finally, in order to ensure that the amounts of hydrogen can be compressed w.r.t. the amount of flow, in these three test sets each turbo compressor in the original natural gas instance is replaced by four parallel hydrogen compressors.

4.2 Computational Setup

We performed our computations on a cluster of machines composed of two *Intel Xeon Gold 5122* running at 3.60 GHz, which provide in total 8 cores and 96 GB of RAM. As solver for the underlying MILP problems we used *Gurobi* in version 9.0.0 [GO20], which was accessed via the native C interface. Since the MILP and LP models turned out to be numerically challenging, we set the *NumericFocus* parameter to the maximum value and used standard settings otherwise. Furthermore, we used the rolling horizon heuristic RHH from [HHLK19], which is a primal heuristic in order to find an incumbent prior to the MILP solves. For each of our instances, we set a cumulative time limit including the heuristic for each tri-level MILP solve to 24 h (86,400 s). If no feasible solution without any slacks was found within the first iteration, we added another 24 h in order to determine a feasible solution with flow slack. Furthermore, besides the Δ-criterion, Algorithm 2 was additionally terminated if the complete run time had exceeded 24 h, which was checked after each IVAP run. For the IVAP, no time limit was imposed.

4.3 Results

The detailed results of our experiments, including the run times, the usage of slack, the number of simple state changes, the energy consumption, and the number of iterations of Algorithm 2, can be found in the Appendix. In this subsection, we summarize them and state the main observations and results. Table 3 summarizes the main characteristics of the five test sets w.r.t. feasibility, network control and compression energy consumption.

First, we focus on the performance of the algorithm and the question whether the test sets were successfully solved. For all instances in the `CH4` test set a solution without any slack was determined by the algorithm. Further, Algorithm 2 terminated with zero optimality gap for the tri-level MILP solves for all instances in `CH4` within 1,800 seconds except for instances 6-1200, 6-1230, 6-1400, and 6-2300. For these four instances, additional iterations had to be performed, i.e., at least one no-good-cut was added, and all have nonzero objectives because of

Test Set	No slack and gap	SS+FD	Energy	Nonzero Gap	Inflow Slack
CH4	333	0.06	345	0	0
H2	332	0.29	278	0	1
H2-12	216	1.1	539	18	98
H2-34	158	1.3	1116	31	170
H2-EQ	111	1.8	1759	70	209

Table 3. Summary of the computational results. While the first column states the test set, the second denotes the number of instances for which the tri-level MILP was solved to optimality and no slack was needed. The third column denotes the average number of simultaneous simple state and flow direction changes. Additionally, in the Energy column, the average compression energy consumption in MWh is depicted. Note that the latter two metrics are w.r.t. to the subset of instances from the first column, i.e., instances with no slack and gap. Finally, the fifth and sixth column denotes the number of instances that terminated with nonzero gap and nonzero inflow slack, respectively.

a simple state change. For test set H2 only one instance, 4-0200, needed small amounts of inflow slack and all but the three instances, 3-0800, 3-0830, and 3-2000, all featuring two simple state changes, terminated within 1800 seconds.

Additionally, for both test sets CH4 and H2, the IVAP terminated successfully for all instances, i.e., a solution being feasible for constraints (M) instead of (7) was found. Thereby, 15 no-good-cuts, i.e., additional iterations of Algorithm 2, were added to 11 instances in total for CH4, while for H2 all runs terminated after the first iteration of the algorithm, i.e., no no-good-cuts were added. Hence, we conclude that the proposed algorithmic approach stated as Algorithm 2 works well on these two test sets.

Next, we discuss the results for the other three test sets. First of all, the number of instances that need flow slacks increases from H2-12 over H2-34 to H2-EQ. However, independent of the test set for none of the instances inflow pressure slacks needed to be applied. Additionally, the solving routine for the tri-level MILP did not terminate within the imposed time limits for an increasing number of instances over the three set sets, i.e., they finished with nonzero gap. Likewise, the solving times of Algorithm 2 increase significantly. For H2-12 44, for H2-34 41, and for H2-EQ 114 instances ran for more than 10,000 seconds. On one hand, the increase in run times can be explained by the increased need for technical measures and the usage of slack. Because of these two factors, proving optimality for an incumbent solution takes longer or cannot be done by the solver. On the other hand, the solver is often not able to either determine a feasible solution or to prove infeasibility for the MILP without slacks within the time limit.

For test set H2-12, the IVAP did not succeed only on instance 6-1030, even after adding the maximum number of 150 no-good-cuts. Here, the initial LP in its very first iteration turns out to be always infeasible. However, for all other instances in this test set the IVAP succeeded and only for two instances an additional iteration of Algorithm 2 was preformed. For the other two test sets, the IVAP failed on more instances: On 21 for H2-34 and on 10 for H2-EQ. This

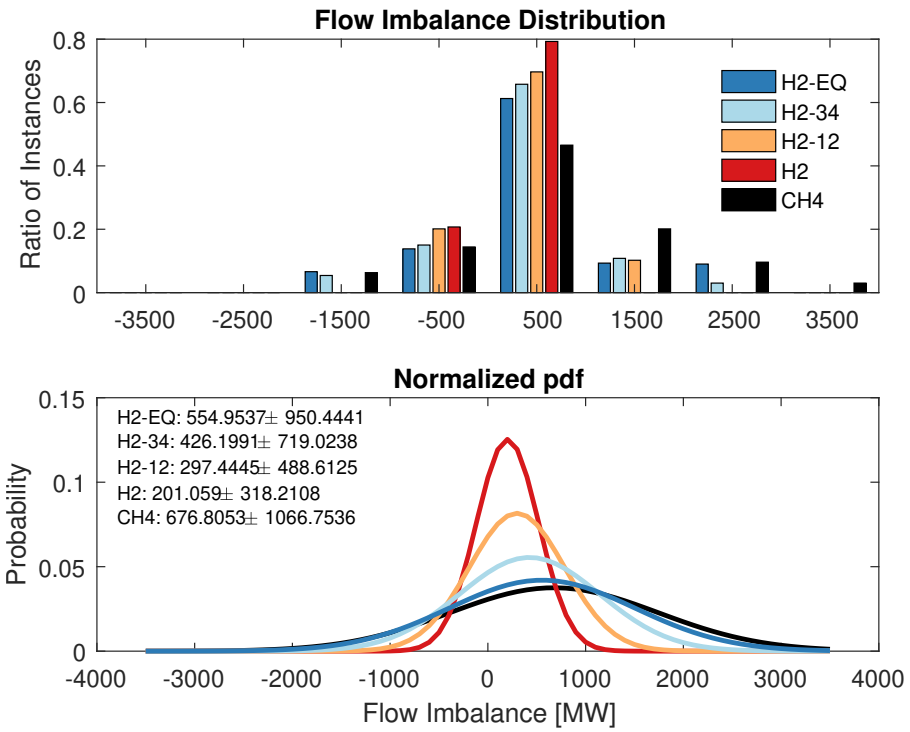

Fig. 1. Distribution of flow imbalances for all test sets. In the upper diagram, the instances of the different test sets are grouped by imbalance intervals where the x-axis ticks depict their centers, while the ratio of contained instances is represented by the y-axis. In the lower diagram the corresponding probability density functions fitted by normal distributions are depicted. Note that probability values are considerably lower than the ratios due to an increase to 71 intervals for smooth normal distribution fits. In the upper left hand corner the mean and standard deviations for the different test sets are shown.

may be due to more significant differences between the gas velocities fixed in the Momentum Equations and the actual gas velocities induced by the corresponding solution. However, a deeper investigation is necessary.

To analyze the reasons for the increasing need for inflow slack over the three test sets `H2-12`, `H2-34`, and `H2-EQ`, we consider the energy imbalance of the instances. This entity we define as

$$\sum_{t\in\mathcal{T}}(\tau(t)-\tau(t-1))\left(\sum_{v\in\mathcal{V}^+}D_{v,t}+\sum_{v\in\mathcal{V}^-}D_{v,t}\right).$$

Figure 1, displays considerable differences in the flow imbalances for the five test sets. Note that although the energy imbalance in the last 12 hours between `CH4` and `H2-EQ` is zero by the test set design, differences exist over the full time

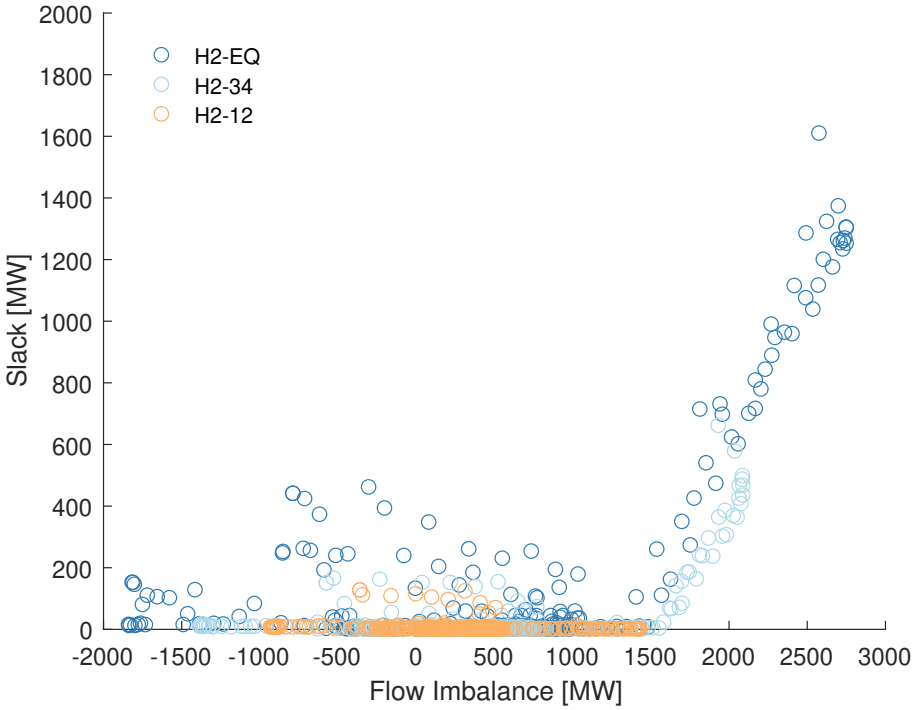

Fig. 2. Scatter plot displaying the flow slack in MW (y-axis) with respect to the flow imbalance in MW (x-axis) for each instance of `H2-12` (orange circles), `H2-34` (light blue circles), and `H2-EQ` (dark blue circles).

horizon of the instances due to the ramp-up procedure we applied. Overall, many scenarios feature a positive flow imbalance, i.e., have more in- than outflow, even for `CH4`. This is due to several factors. First, the real-world based data does not account for fuel gas used for compression. Second, regulation demands that in- and outflows only have to be balanced within the time window from 6am to 6am. However, in practice this rule is not strictly enforced by the transport system operators for operational reasons. Finally, although we performed several consistency checks, we cannot guarantee perfect accuracy of the data, since it originates from past real-world measurements.

Next, we investigate the connection between the flow imbalances of the instances of the `H2-12`, `H2-34` and the `H2-EQ` test sets and the total slack in the corresponding solutions (Figure 2). The slack for `H2-12` and `H2-34` is typically small and is independent for flow imbalance values in the range of -1500 to 1500 MW. In this range we observe instances that need flow slack despite of no or only small flow imbalances. A deeper analysis revealed, that in some parts of the network, which are disconnected from major transport pipelines as well as major sources or sinks by the network control, there are local flow imbalances. Due to the scaling procedure, these local phenomena become more severe, such that

Test Set	SS+FD	Energy
CH4	0.1	380
H2	0.5	300
H2-12	1.3	536
H2-34	1.4	1074
H2-EQ	1.8	1753

Table 4. Summary of the results for the instances that were solved with zero gap and no slack in each of the five test sets. SS+FD denotes the average number of control measures and Energy the average compressor energy consumption in MWh.

inflow slack needs to be applied in order to respect the (inflow) pressure bounds, too. Apparently, the model is not able to determine a way to balance these local phenomena using simple state changes. However, for test set H2-34 as well as for test set H2-EQ we observe that the necessary slack scales linearly starting from an imbalance of about 1,500 MW. Here, the network is not able to transport the inserted amount of gas away from the entries such that the pressure would increase and violate (inflow) pressure bounds if no slack is applied.

Additionally, we recall that we start from an initial state that originates from natural gas transport. Thus, we implicitly impose that the transport of hydrogen would also allow for or utilize such a network state. Therefore, some slack may also be due to the adaption process to a different style of network control.

Overall, we conclude that a realization of transport seems to be possible in a majority of the scenarios, including those in test set H2-EQ for which in- and outflows are balanced. For most other instances from H2-12, H2-34, and H2-EQ, which are balanced but need some small inflow slacks, a control without inflow slack may be possible after a revision of the network stations.

Finally, we compare the characteristics of the successful instances without slack and with zero gap in terms of control measures and energy needed for compression. Regarding control measures we focus on simple state changes that were performed with simultaneous flow direction changes (SS+FD, cf. Table 3). Hence, we do not simply count simple state changes, as most of them correspond to simply switching on compressing arcs and do not indicate any actual difference w.r.t. the flow patterns. Instead, we regard a simple state change as a control measure in our analysis only if a flow direction change is performed simultaneously. The compression energy is determined in a post processing using the actual power equation. In this analysis, we only consider those 110 instances, which were solved in all test sets without any slack and zero gap. Note that in contrast to the subset analyzed here and visualized Figure 3, the averages in Table 3 are based on all successful instances of the respective test sets.

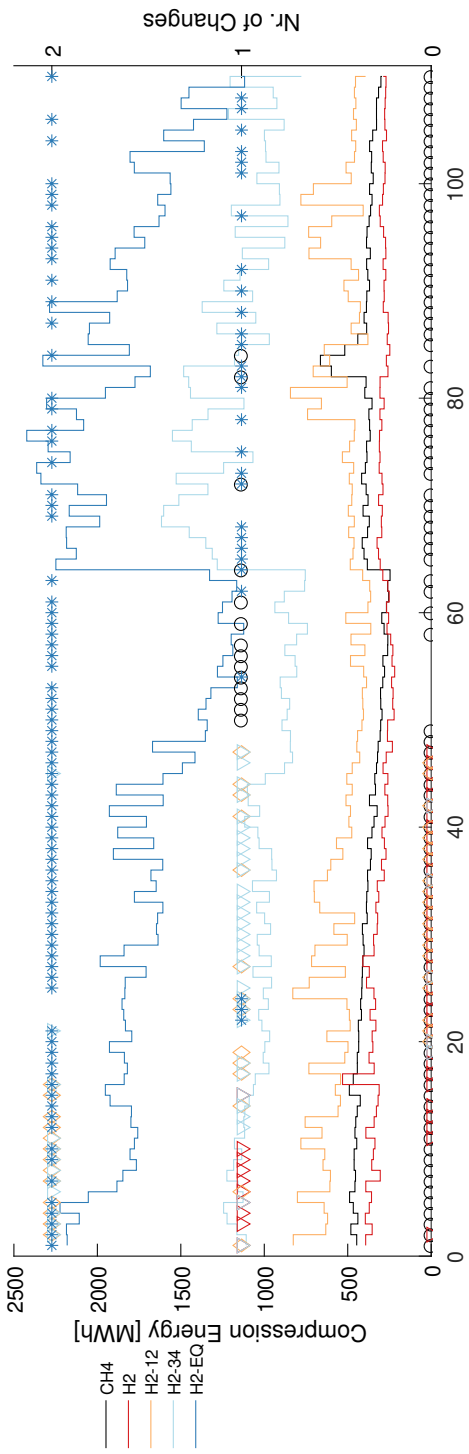

Fig. 3. Comparison of compression energy and SS+FD in successful instances. On the x-axis, the subset of instances solved with zero gap and no slack in all test sets are displayed in chronological order. The colored curves together with the left hand side y-axis show the amount of energy used for compression. The symbols scaled to the right hand side y-axis show the number of simple state changes, which were conducted together with a flow direction change.

The first observation is that more compression energy is needed for instances with higher in- and outflows. $3.64 \pm 0.6(1\sigma)$ times more energy is needed in the instances of `H2-EQ` compared to `CH4`. Note, that the proposed algorithm does not optimize the control w.r.t. the amount of compression energy needed. Thus, conducting different technical control measures leads to different compression patterns and thereby a varying energy consumption. Likewise, with increasing supplies and demands, more technical control measures become necessary. While for `CH4` and `H2` rarely one control measure needs to be applied, for `H2-EQ` we mostly have two combined simple state and flow direction changes (cf. Table 3). Since we ensured that compression is possible by installing the necessary number of hydrogen compressors, we conclude that the increased need for technical control measures to satisfy supplies and demands is due to the reduced linepack w.r.t. energy.

5 Conclusion

Our feasibility study on whether an existing gas transport network can be converted to a pure hydrogen transport network w.r.t. its control yields promising results and gives a positive answer provided that certain technical and regulatory conditions are fulfilled. However, before we state our conclusion regarding the computational study and the presented algorithmic approach for the robust operation of hydrogen transport networks in more detail, we add a disclaimer.

First, the instances used in our experiments are based on about two weeks of measured data from a real-world natural gas transport network. Thus, besides not being able to guarantee perfect accuracy and consistency, there may exist other transport scenarios which could turn out to be more difficult for hydrogen transport when converted. To the best of our knowledge, there does not exist any data for real-world large-scale hydrogen transport networks, since they do not exist yet. Therefore, we converted natural gas scenarios in a way, which we assume to be reasonable. Additionally, we have to keep in mind that the initial state originates from natural gas transport. Thus, we implicitly impose that hydrogen transport would allow for or even utilize such a state in everyday operations, which we cannot know for sure. All that being said, our feasibility study on whether a current natural gas transport network can be transformed into a pure hydrogen network revealed several important results.

First of all, without a replacement of the currently installed turbo compressors by hydrogen compressors, which comprise multiple serial compression stages, transport is not possible even for test set `H2`, as preliminary experiments indicated. This is due to the drastically reduced maximum compression ratio of turbo compressor machines for hydrogen, see for example the rule of thumb given as equation (8). Additionally, as we need to transport more than three times the amount of volumetric flow in energy equivalent scenarios, an installation of additional parallel hydrogen compressors becomes necessary as well.

However, our analysis shows that a realization of transport seems to be possible for a majority of instances when in- and outflows are nearly balanced, i.e.,

when in- and outflow into the network do not differ too much over time. Thus, one may suggest to impose stricter regulatory measures for hydrogen transport, for example to force gas traders to balance their in- and outflows within 12 or less hours compared to the 24 in natural gas transport.

Next, with increasing supplies and demands, more technical control measures become necessary. For `H2-EQ` at least one simultaneous simple state and flow direction change is performed for each instance, while for `H2` none is necessary for a majority of scenarios. This indicates that due to the reduced linepack the network control has to become more dynamic. Additionally, we find that the energy needed for compression increases by 364% on average compared to natural gas.

Finally, regarding the algorithmic approach itself, considering the promising results for test sets `H2` and `H2-12`, we conclude that it represents a valuable basis for further development regarding a decision-support-system for the transport of hydrogen similar to [HHLK19]. As the control of the network becomes more dynamic, such a tool can be of great help to the dispatchers. Still, to overcome the usage of small inflow slack amounts due to the imbalances in disconnected subnetworks, we need to conduct a deeper investigation and revision of adjacent network stations, in order to allow for a control equalizing it.

Acknowledgement

The work for this article has been conducted in the Research Campus MODAL funded by the German Federal Ministry of Education and Research (BMBF) (fund numbers 05M14ZAM, 05M20ZBM).

References

AAB+13. Jean André, Stéphane Auray, Jean Brac, Daniel De Wolf, Guy Maisonnier, Mohamed-Mahmoud Ould-Sidi, and Antoine Simonnet. Design and dimensioning of hydrogen transmission pipeline networks. *European Journal of Operational Research*, 229(1):239–251, 2013.

Ada20. Adam, Peter and Engelshove, Stefan and Heunemann, Frank and Thiemann, Thomas and von dem Busche, Christoph. Hydrogen infrastructure - the pillar of energy transition. Technical report, Siemens Energy, Gascade Gastransport GmbH, Nowega GmbH, 2020. Accessed on 26.10.2020.

BEG+19. Robert Burlacu, Herbert Egger, Martin Groß, Alexander Martin, Marc Pfetsch, Lars Schewe, Mathias Sirvent, and Martin Skutella. Maximizing the storage capacity of gas networks: A global MINLP approach. *Optimization and Engineering*, 20(2):543–573, June 2019.

BGG+13. Sylvestre Baufumé, Fabian Grüger, Thomas Grube, Dennis Krieg, Jochen Linssen, Michael Weber, Jürgen-Friedrich Hake, and Detlef Stolten. GIS-based scenario calculations for a nationwide German hydrogen pipeline infrastructure. *International Journal of Hydrogen Energy*, 38(10):3813–3829, 2013.

BS79. Sita Bhaskaran and Franz J.M. Salzborn. Optimal design of gas pipeline networks. *Journal of the Operational Research Society*, pages 1047–1060, 1979.

C$^+$92. Günter Cerbe et al. Grundlagen der Gastechnik. *Gasbeschaffung, Gasverteilung, Gasverwendung*, 5, 1992.

DD13. Paul E Dodds and Stephanie Demoullin. Conversion of the UK gas system to transport hydrogen. *International Journal of Hydrogen Energy*, 38(18):7189–7200, 2013.

DG16. Markus G. Drouven and Ignacio E. Grossmann. Multi-period planning, design and strategic models for long-term, quality-sensitive shale gas development. *AIChE Journal*, 2016.

DGK$^+$11. Pia Domschke, Björn Geißler, Oliver Kolb, Jens Lang, Alexander Martin, and Antonio Morsi. Combination of Nonlinear and Linear Optimization of Transient Gas Networks. *INFORMS Journal on Computing*, 23(4):605–617, 2011.

Die20. Die Bundesregierung. Die Nationale Wasserstoffstrategie. Bundesministerium für Wirtschaft und Energie (BMWi), 2020. Accessed on 12.06.2020.

FGG$^+$15. Armin Fügenschuh, Björn Geißler, Ralf Gollmer, Antonio Morsi, Marc E. Pfetsch, Jessica Rövekamp, Martin Schmidt, Klaus Spreckelsen, and Marc C. Steinbach. Physical and technical fundamentals of gas networks. In Koch et al. [KHPS15].

GLM$^+$18. Martin Gugat, Günter Leugering, Alexander Martin, Martin Schmidt, Mathias Sirvent, and David Wintergerst. MIP-based instantaneous control of mixed-integer PDE-constrained gas transport problems. *Computational Optimization and Applications*, 70(1):267–294, May 2018.

GO20. LLC Gurobi Optimization. Gurobi Optimizer Reference Manual, Version 9.0. http://www.gurobi.com, 2020.

Gro19. Markus Groissböck. Are open source energy system optimization tools mature enough for serious use? *Renewable and Sustainable Energy Reviews*, 102:234–248, 2019.

HAH$^+$19. Felix Hennings, Lovis Anderson, Kai Hoppmann, Mark Turner, and Thorsten Koch. Controlling transient gas flow in real-world pipeline intersection areas. Technical Report 19-24, ZIB, Takustr. 7, 14195 Berlin, 2019.

HD07a. Dries Haeseldonckx and William D'haeseleer. The use of the natural-gas pipeline infrastructure for hydrogen transport in a changing market structure. *International Journal of Hydrogen Energy*, 32(10):1381 – 1386, 2007. EHEC2005.

HD07b. Dries Haeseldonckx and William D'haeseleer. The use of the natural-gas pipeline infrastructure for hydrogen transport in a changing market structure. *International Journal of Hydrogen Energy*, 32(10-11):1381–1386, 2007.

Hen18. Felix Hennings. Benefits and Limitations of Simplified Transient Gas Flow Formulations. In *Operations Research Proceedings 2017*, pages 231–237. Springer, 2018.

HHLK19. Kai Hoppmann, Felix Hennings, Ralf Lenz, and Thorsten Koch. Optimal Operation of Transient Gas Transport Networks. Technical Report 19-23, ZIB, Takustr. 7, 14195 Berlin, 2019.

Hum17. Jesco Humpola. *Gas network optimization by MINLP*. Logos Verlag Berlin GmbH, 2017.

KHPS15. Thorsten Koch, Benjamin Hiller, Marc E. Pfetsch, and Lars Schewe, editors. *Evaluating Gas Network Capacities*, volume 21 of *MOS-SIAM Series on Optimization*. SIAM, 2015.

KLB10. Oliver Kolb, Jens Lang, and Pia Bales. An Implicit Box Scheme for Subsonic Compressible Flow with Dissipative Source Term. *Numerical Algorithms*, 53(2-3):293–307, 2010.

Mor07. Susanne Moritz. *A Mixed Integer Approach for the Transient Case of Gas Network Optimization*. PhD thesis, Technische Universität Darmstadt, Darmstadt, 2007.

MVHZ+16. Terrence WK Mak, Pascal Van Hentenryck, Anatoly Zlotnik, Hassan Hijazi, and Russell Bent. Efficient dynamic compressor optimization in natural gas transmission systems. In *American Control Conference (ACC), 2016*, pages 7484–7491. IEEE, 2016.

Nik50. Johann Nikuradse. *Laws of Flow in Rough Pipes*. National Advisory Committee for Aeronautics Washington, 1950.

ORG+17. A. Otto, M. Robinius, T. Grube, S. Schiebahn, A. Praktiknjo, and D. Stolten. Power-to-Steel: Reducing CO_2 through the Integration of Renewable Energy and Hydrogen into the German Steel Industry. *Energies*, 10(451), 2017.

Osi96. Andrej J. Osiadacz. Different Transient Flow Models - Limitations, Advantages, And Disadvantages. In *PSIG-9606*. Pipeline Simulation Interest Group, 1996.

Pap68. Papay. A termeléstechnológiai paraméterek változása a gáztelepek muvelése során. *OGIL Musz. Tud. Kozl.*, 1968.

RFR+70. B. Rothfarb, H. Frank, D.M. Rosenbaum, K. Steiglitz, and D.J. Kleitman. Optimal design of offshore natural-gas pipeline systems. *Operations Research*, 18(6):992–1020, 1970.

RGRS19. Markus Reuß, Thomas Grube, Martin Robinius, and Detlef Stolten. A hydrogen supply chain with spatial resolution: Comparative analysis of infrastructure technologies in Germany. *Applied Energy*, 247:438–453, 2019.

RWT+19. Markus Reuß, Lara Welder, Johannes Thürauf, Jochen Linßen, Thomas Grube, Lars Schewe, Martin Schmidt, Detlef Stolten, and Martin Robinius. Modeling hydrogen networks for future energy systems: A comparison of linear and nonlinear approaches. *International Journal of Hydrogen Energy*, 44(60):32136–32150, 2019.

SSS16. Sheila Samsatli, Iain Staffell, and Nouri J Samsatli. Optimal design and operation of integrated wind-hydrogen-electricity networks for decarbonising the domestic transport sector in Great Britain. *International Journal of Hydrogen Energy*, 41(1):447–475, 2016.

WP18. Alexandra C Weber and Lazaros G Papageorgiou. Design of hydrogen transmission pipeline networks with hydraulics. *Chemical Engineering Research and Design*, 131:266–278, 2018.

YO07. Christopher Yang and Joan Ogden. Determining the lowest-cost hydrogen delivery mode. *International Journal of Hydrogen Energy*, 32(2):268–286, 2007.

ZCB15. Anatoly Zlotnik, Michael Chertkov, and Scott Backhaus. Optimal control of transient flow in natural gas networks. In *54th IEEE Conference on Decision and Control (CDC)*, pages 4563–4570. IEEE, 2015.

Appendix

Weights and Parameters

Here, we state the weights and parameters for the different algorithmic components used in Algorithm 2.

First, for the tri-level MILP we used the following weights and parameters: The cost parameters regarding the third level objective were set to $w^a = 5.0$ for all $a \in \mathcal{A}^{\text{ar}}$ and for each simple state $s \in \mathcal{S}$ an individual cost $w^s \in \{0, \dots, 200\}$ for a change into it was fixed according to expert opinions. The cost for both types of slack variables is equal to 1.0, see Section 3.4.

Next, for the solution smoothing from Subsection 3.5, which is explained in detail in [HHLK19], we used $w_v^{\text{sm-q}} := 13$, $w_v^{\text{sm-p}} := 1300$, $w_i^{\text{sm-q}} := |\mathcal{V}_i^{\text{fn}}|$, and $w_i^{\text{sm-p}} := 100.0|\mathcal{V}_i^{\text{fn}}|$ for each $v \in \mathcal{V}_i^{\text{fn}}$ in network station G_i.

Next, for the IVAP we used $\overline{w}^{\text{sm-p}} := 10^4$, $w_v^{\text{sm-p}} := 1$ for all $v \in \mathcal{V}^{\text{pi}}$, $\overline{w}^{\text{sm-q}} := 10^3$, and $w_v^{\text{sm-q}} := 1$ for all $v \in \mathcal{V}^{\text{pi}}$ and the parameters $\varepsilon := 10^{-2}\frac{m}{s}$, $k = 3$, and $\Delta = 150$. Additionally, we decrease the threshold value v^{min}, which is used to determine the fixed absolute velocity value in the Momentum Equation constraints (7) to $10^{-3}\frac{m}{s}$.

Results for test set `CH4`

The columns of the following tables contain the results of the computational experiments for test set `CH4` described and discussed in Section 4. Here, the first column contains the instance name. It consists of the virtual day together with the time in hours and minutes of the corresponding initial state, i.e., 2-0400 is the instance having the initial state from 4am of virtual day 2. The second column states the run time of the complete algorithmic approach Algorithm 2 for the corresponding instance until it was terminated. While the third column denotes the total number of conducted simple state changes, the fourth column accounts only for those in which a flow direction change was performed simultaneously. Next, the fifth column states the amount of compression energy that was used in MWh. Finally, while the sixth column denotes the flow imbalance in kg, the last column states the number of iterations of Algorithm 2, which is equivalent to the number of added no-good-cuts.

Instance	Runtime	SS	SS+FD	Energy	Imbalance	Alg-Iter
1-1200	144	0	0	446	937 587	0
1-1230	307	0	0	481	957 877	0
1-1300	156	0	0	439	1 150 775	0
1-1330	157	0	0	467	1 372 272	0
1-1400	159	0	0	489	1 450 230	0
1-1430	354	0	0	457	1 469 730	0
1-1500	144	0	0	453	1 637 187	0
1-1530	307	0	0	462	1 665 136	0
1-1600	172	0	0	462	1 787 531	0

Instance	Runtime	SS	SS+FD	Energy	Imbalance	Alg-Iter
1-1630	290	0	0	449	1 838 633	0
1-1700	253	0	0	446	1 828 104	0
1-1730	242	0	0	457	1 824 838	0
1-1800	166	0	0	452	1 757 738	0
1-1830	152	0	0	443	1 725 303	0
1-1900	166	0	0	425	1 640 375	0
1-1930	238	0	0	490	1 605 609	0
1-2000	247	0	0	479	1 490 590	0
1-2030	269	0	0	467	1 430 600	0
1-2100	248	0	0	442	1 314 478	0
1-2130	229	0	0	443	1 256 009	0
1-2200	245	0	0	431	1 113 943	0
1-2230	161	0	0	434	1 071 276	0
1-2300	240	0	0	434	963 572	0
1-2330	179	0	0	436	925 870	0
2-0000	149	0	0	411	865 785	0
2-0030	253	0	0	418	825 357	0
2-0100	248	0	0	423	747 585	0
2-0130	255	0	0	416	712 351	0
2-0200	237	0	0	404	647 573	0
2-0230	253	0	0	414	624 758	0
2-0300	296	0	0	412	529 154	0
2-0330	301	0	0	410	477 770	0
2-0400	338	0	0	415	370 497	0
2-0430	317	0	0	402	310 279	0
2-0500	318	0	0	408	156 607	0
2-0530	282	0	0	412	127 120	0
2-0600	143	0	0	400	84 815	0
2-0630	136	0	0	383	96 127	0
2-0700	156	0	0	388	198 562	0
2-0730	179	0	0	386	247 899	0
2-0800	203	0	0	377	353 511	0
2-0830	148	0	0	379	422 181	0
2-0900	168	0	0	381	462 583	0
2-0930	154	0	0	364	496 565	0
2-1000	209	0	0	388	664 575	0
2-1030	158	0	0	359	664 042	0
2-1100	244	0	0	381	644 885	0
2-1130	155	0	0	355	624 691	0

Instance	Runtime	SS	SS+FD	Energy	Imbalance	Alg-Iter
2-1200	219	0	0	371	651 113	0
2-1230	160	0	0	342	647 577	0
2-1300	161	0	0	324	700 762	0
2-1330	829	0	0	370	672 938	0
2-1400	185	0	0	339	704 869	0
2-1430	207	0	0	334	703 785	0
2-1500	195	0	0	340	735 565	0
2-1530	239	0	0	338	709 579	0
2-1600	172	0	0	325	680 715	0
2-1630	171	0	0	328	700 938	0
2-1700	318	0	0	321	738 743	0
2-1730	180	0	0	318	728 191	0
2-1800	173	0	0	314	464 387	0
2-1830	189	0	0	306	360 858	0
2-1900	184	0	0	292	235 634	0
2-1930	177	0	0	303	194 344	0
2-2000	313	1	1	294	141 549	0
2-2030	1739	1	1	302	117 106	0
2-2100	1011	1	1	303	26 774	0
2-2130	1257	1	1	290	−15 695	0
2-2200	320	1	1	279	−108 674	0
2-2230	420	1	1	289	−152 307	0
2-2300	229	1	1	261	−291 601	0
2-2330	239	1	1	260	−328 056	0
3-0000	228	0	0	282	−409 889	0
3-0030	569	1	1	296	−419 117	0
3-0100	300	0	0	268	−461 657	0
3-0130	661	1	1	255	−478 710	0
3-0200	191	0	0	256	−520 195	0
3-0230	423	1	1	265	−534 862	0
3-0300	281	0	0	261	−533 922	0
3-0330	164	0	0	246	−534 444	0
3-0400	192	0	0	266	−536 085	0
3-0430	527	1	1	273	−545 080	0
3-0500	164	0	0	273	−568 726	0
3-0530	352	0	0	252	−578 520	1
3-0600	155	0	0	262	−620 311	0
3-0630	209	0	0	269	−643 576	0
3-0700	168	0	0	281	−786 552	0
3-0730	149	0	0	245	−880 228	0
3-0800	141	0	0	258	−1 026 394	0
3-0830	142	0	0	258	−1 026 394	0
3-0900	167	0	0	264	−1 205 227	0
3-0930	159	0	0	268	−1 233 964	0
3-1000	211	0	0	292	−1 051 462	0
3-1030	199	0	0	286	−917 114	0
3-1100	170	0	0	285	−803 867	0
3-1130	228	0	0	231	−711 773	0

Instance	Runtime	SS	SS+FD	Energy	Imbalance	Alg-Iter
3-1200	180	0	0	219	−536 546	0
3-1230	230	0	0	236	−397 205	0
3-1300	159	0	0	237	−276 225	0
3-1330	195	0	0	217	−200 417	0
3-1400	186	0	0	220	−163 930	0
3-1430	181	0	0	221	−104 913	0
3-1500	160	0	0	223	−15 604	0
3-1530	164	0	0	220	29 308	0
3-1600	148	0	0	233	69 446	0
3-1630	173	0	0	231	73 285	0
3-1700	176	0	0	228	100 714	0
3-1730	137	0	0	216	145 056	0
3-1800	165	0	0	221	409 485	0
3-1830	139	0	0	214	549 527	0
3-1900	173	0	0	218	672 859	0
3-1930	170	0	0	214	739 446	0
3-2000	177	0	0	217	816 256	0
3-2030	171	0	0	280	892 373	0
3-2100	172	1	0	260	1 024 963	0
3-2130	173	1	1	276	1 078 579	0
3-2200	322	1	1	265	1 204 527	0
3-2230	183	1	0	243	1 286 348	0
3-2300	153	0	0	284	1 461 524	0
3-2330	142	0	0	248	1 511 868	0
4-0000	177	0	0	253	1 622 832	0
4-0030	140	0	0	255	1 606 114	0
4-0100	155	0	0	233	1 590 899	0
4-0130	145	0	0	238	1 561 612	0
4-0200	152	0	0	220	1 527 549	0
4-0230	147	0	0	252	1 474 785	0
4-0300	184	0	0	227	1 429 830	0
4-0330	153	0	0	242	1 402 420	0
4-0400	157	0	0	199	1 395 894	0
4-0430	177	0	0	223	1 396 321	0
4-0500	142	0	0	239	1 389 218	0
4-0530	147	0	0	218	1 326 282	0
4-0600	146	0	0	234	1 254 206	0
4-0630	165	0	0	229	1 267 305	0
4-0700	151	0	0	232	1 448 212	0
4-0730	145	0	0	226	1 504 836	0
4-0800	161	0	0	224	1 561 978	0
4-0830	164	0	0	234	1 499 749	0
4-0900	147	0	0	249	1 304 440	0
4-0930	158	0	0	248	1 085 166	0
4-1000	160	0	0	255	588 151	0
4-1030	172	0	0	251	306 108	0
4-1100	163	0	0	253	−42 758	0
4-1130	166	0	0	275	−283 713	0

Instance	Runtime	SS	SS+FD	Energy	Imbalance	Alg-Iter
4-1200	220	0	0	279	−686 161	0
4-1230	163	0	0	285	−991 019	0
4-1300	171	0	0	277	−1 361 054	0
4-1330	184	0	0	307	−1 574 419	0
4-1400	206	0	0	315	−1 792 112	0
4-1430	186	0	0	336	−1 941 797	0
4-1500	167	0	0	308	−2 156 480	0
4-1530	195	0	0	343	−2 224 473	0
4-1600	196	0	0	353	−2 327 456	0
4-1630	219	0	0	348	−2 387 498	0
4-1700	191	0	0	384	−2 548 052	0
4-1730	225	0	0	339	−2 694 243	0
4-1800	182	0	0	376	−2 824 433	0
4-1830	215	0	0	416	−2 893 266	0
4-1900	215	0	0	419	−2 973 482	0
4-1930	183	0	0	405	−3 008 679	0
4-2000	242	0	0	416	−3 027 965	0
4-2030	211	0	0	460	−3 046 369	0
4-2100	224	0	0	471	−3 048 737	0
4-2130	207	0	0	397	−3 015 735	0
4-2200	192	0	0	454	−3 020 750	0
4-2230	212	0	0	502	−2 992 784	0
4-2300	201	0	0	534	−2 959 635	0
4-2330	209	0	0	526	−2 957 380	0
6-0000	266	1	1	383	−412 131	0
6-0030	210	0	0	402	−380 339	0
6-0100	374	0	0	413	−380 498	0
6-0130	209	1	0	381	−293 519	0
6-0200	434	1	0	371	−293 744	0
6-0230	229	0	0	408	−13 376	0
6-0300	341	0	0	378	−13 376	0
6-0330	408	1	0	390	191 599	0
6-0400	271	1	1	417	191 127	0
6-0430	241	0	0	394	148 350	0
6-0500	201	0	0	385	148 495	0
6-0530	215	1	0	387	189 638	0
6-0600	433	1	0	365	189 611	0
6-0630	204	0	0	369	152 315	0
6-0700	190	0	0	368	218 470	0
6-0730	379	1	0	373	396 488	0
6-0800	291	1	0	354	397 666	0
6-0830	214	0	0	377	536 175	0
6-0900	213	0	0	380	535 759	0
6-0930	458	1	0	399	734 803	0
6-1000	411	1	1	387	737 781	0
6-1030	234	0	0	398	748 308	0
6-1100	290	0	0	390	748 169	2
6-1130	273	1	0	398	694 453	1

Instance	Runtime	SS	SS+FD	Energy	Imbalance	Alg-Iter
6-1200	8923	1	1	574	623 878	1
6-1230	2973	1	0	544	581 705	2
6-1300	357	1	1	598	531 697	0
6-1330	323	1	1	565	467 111	0
6-1400	4175	1	0	664	361 884	2
6-1430	307	1	1	518	297 829	0
6-1500	249	0	0	440	361 819	0
6-1530	318	0	0	387	523 938	0
6-1600	237	0	0	402	793 081	0
6-1630	336	0	0	388	964 266	0
6-1700	196	0	0	399	1 169 320	0
6-1730	228	0	0	409	1 290 086	0
6-1800	222	0	0	394	1 492 078	0
6-1830	329	1	0	394	1 568 530	0
6-1900	182	1	0	400	1 662 643	0
6-1930	298	1	0	411	1 657 723	0
6-2000	646	2	0	408	1 639 946	2
6-2030	232	1	0	415	1 676 963	0
6-2100	270	1	0	416	1 732 251	0
6-2130	266	1	0	418	1 798 113	1
6-2200	255	1	0	422	1 906 519	0
6-2230	281	1	0	419	1 944 444	1
6-2300	10 524	1	0	431	1 992 298	1
6-2330	160	0	0	435	1 992 582	1
7-0000	182	0	0	435	1 959 515	0
7-0030	174	0	0	440	1 903 422	0
7-0100	179	0	0	433	1 774 190	0
7-0130	170	0	0	437	1 696 005	0
7-0200	180	0	0	442	1 586 070	0
7-0230	186	0	0	438	1 526 365	0
7-0300	240	0	0	443	1 441 760	0
7-0330	251	0	0	453	1 400 022	0
7-0400	228	0	0	458	1 370 517	0
7-0430	209	0	0	443	1 426 812	0
7-0500	264	0	0	460	1 529 520	0
7-0530	228	0	0	461	1 547 471	0
7-0600	212	0	0	464	1 584 125	0
7-0630	167	0	0	436	1 556 584	0
7-0700	234	0	0	453	1 509 339	0
7-0730	229	0	0	475	1 503 959	0
7-0800	186	0	0	445	1 487 131	0
7-0830	203	0	0	455	1 473 261	0
7-0900	248	0	0	445	1 478 892	0
7-0930	224	0	0	450	1 439 741	0
7-1000	231	0	0	480	1 434 509	0
7-1030	214	0	0	448	1 536 512	0
7-1100	220	0	0	469	1 682 756	0
7-1130	278	0	0	460	1 753 300	0

Instance	Runtime	SS	SS+FD	Energy	Imbalance	Alg-Iter
7-1200	203	0	0	438	1 847 006	0
7-1230	216	0	0	443	1 854 046	0
7-1300	253	0	0	452	1 854 363	0
7-1330	436	0	0	451	1 862 676	0
7-1400	224	0	0	449	1 830 463	0
7-1430	217	0	0	439	1 833 944	0
7-1500	228	0	0	439	1 787 920	0
7-1530	192	0	0	436	1 754 936	0
7-1600	440	0	0	451	1 627 178	0
7-1630	191	0	0	434	1 557 312	0
7-1700	214	0	0	428	1 475 887	0
7-1730	202	0	0	434	1 455 084	0
7-1800	206	0	0	434	1 424 055	0
7-1830	198	0	0	409	1 377 437	0
7-1900	219	0	0	403	1 308 076	0
7-1930	200	0	0	401	1 272 123	0
7-2000	192	0	0	412	1 209 144	0
7-2030	187	0	0	389	1 187 809	0
7-2100	181	0	0	396	1 175 733	0
7-2130	223	0	0	386	1 174 486	0
7-2200	213	0	0	376	1 179 305	0
7-2230	151	0	0	386	1 193 021	0
7-2300	196	0	0	369	1 209 263	0
7-2330	149	0	0	380	1 220 138	0
8-0000	179	0	0	387	1 236 968	0
8-0030	187	0	0	365	1 273 708	0
8-0100	171	0	0	387	1 400 688	0
8-0130	183	0	0	384	1 462 887	0
8-0200	173	0	0	372	1 527 455	0
8-0230	177	0	0	363	1 574 493	0
8-0300	166	0	0	354	1 661 806	0
8-0330	177	0	0	369	1 682 276	0
8-0400	187	0	0	347	1 659 721	0
8-0430	170	0	0	359	1 637 052	0
8-0500	174	0	0	357	1 608 532	0
8-0530	175	0	0	369	1 603 445	0
8-0600	165	0	0	350	1 588 751	0
8-0630	164	0	0	327	1 582 110	0
8-0700	167	0	0	328	1 690 406	0
8-0730	179	0	0	328	1 737 283	0
8-0800	174	0	0	315	1 799 537	0
8-0830	182	0	0	301	1 833 787	0
8-0900	190	0	0	323	1 875 427	0
8-0930	185	0	0	296	1 934 056	0
8-1000	157	0	0	283	2 010 785	0
8-1030	183	0	0	281	2 055 087	0
8-1100	174	0	0	297	2 217 295	0
8-1130	180	0	0	293	2 426 878	0

Instance	Runtime	SS	SS+FD	Energy	Imbalance	Alg-Iter
8-1200	187	0	0	286	2 788 246	0
8-1230	179	0	0	284	3 071 818	0
8-1300	190	0	0	275	3 472 413	0
8-1330	229	0	0	283	3 660 691	0
8-1400	191	0	0	269	3 949 092	0
8-1430	167	0	0	283	4 076 454	0
8-1500	200	0	0	269	4 275 609	0
8-1530	186	0	0	268	4 386 862	0
8-1600	198	0	0	267	4 598 516	0
8-1630	203	0	0	263	4 721 583	0
8-1700	161	0	0	265	4 858 012	0
8-1730	199	0	0	232	4 888 837	0
8-1800	185	0	0	230	4 904 134	0
8-1830	178	0	0	216	4 901 191	0
8-1900	176	0	0	206	4 902 014	0
8-1930	181	0	0	277	4 875 685	0
8-2000	175	0	0	253	4 849 345	0
8-2030	184	0	0	252	4 791 535	0
8-2100	174	0	0	255	4 697 251	0
8-2130	151	0	0	241	4 643 512	0
8-2200	183	0	0	247	4 586 176	0
8-2230	164	0	0	237	4 499 442	0
8-2300	141	0	0	240	4 336 682	0
8-2330	224	0	0	235	4 239 311	0
9-0000	193	0	0	253	4 141 105	0
9-0030	179	0	0	250	4 118 445	0
9-0100	162	0	0	247	4 057 389	0
9-0130	161	0	0	244	4 040 457	0
9-0200	162	0	0	242	4 062 370	0
9-0230	161	0	0	239	4 030 539	0
9-0300	158	0	0	225	3 924 725	0
9-0330	156	0	0	242	3 889 521	0
9-0400	144	0	0	238	3 862 687	0
9-0430	149	0	0	219	3 842 896	0
9-0500	157	0	0	240	3 777 439	0
9-0530	167	0	0	239	3 745 948	0
9-0600	148	0	0	234	3 707 384	0
9-0630	184	0	0	244	3 673 858	0
9-0700	164	0	0	203	3 596 362	0
9-0730	168	0	0	233	3 525 181	0
9-0800	193	0	0	211	3 430 246	0
9-0830	151	0	0	216	3 369 537	0
9-0900	187	0	0	214	3 280 417	0
9-0930	200	0	0	215	3 193 766	0
9-1000	164	0	0	193	3 028 569	0

Results for test set H2

The columns of the following tables contain the results of the computational experiments for test set H2 described and discussed in Section 4. Here, the first column contains the instance name. It consists of the virtual day together with the time in hours and minutes of the corresponding initial state, i.e., 2-0400 is the instance having the initial state from 4am of virtual day 2. The second column states the run time of the complete algorithmic approach Algorithm 2 for the corresponding instance until it was terminated. While the third column denotes the total number of conducted simple state changes, the fourth column accounts only for those in which a flow direction change was performed simultaneously. Next, the fifth column states the amount of compression energy that was used in MWh. Finally, while the sixth column denotes the flow imbalance in kg, the last column states the number of iterations of Algorithm 2, which is equivalent to the number of added no-good-cuts. As we only needed 1299 kg of slack for instance 4-0200, we omit this column for this test set here.

Instance	Runtime	SS	SS+FD	Energy	Imbalance	Alg-Iter
1-1200	127	1	1	392	108 659	0
1-1230	127	1	1	354	111 428	0
1-1300	121	1	1	395	135 055	0
1-1330	121	1	1	371	160 376	0
1-1400	146	1	1	358	169 046	0
1-1430	126	1	1	392	171 421	0
1-1500	123	1	1	305	191 044	0
1-1530	134	1	1	356	194 522	0
1-1600	116	1	1	346	208 731	0
1-1630	128	1	1	337	215 274	0
1-1700	124	1	1	337	212 662	0
1-1730	122	1	1	391	210 074	0
1-1800	128	1	1	342	202 376	0
1-1830	126	1	1	328	198 873	0
1-1900	123	1	1	318	189 331	0
1-1930	121	1	1	312	185 204	0
1-2000	137	2	1	356	172 105	0
1-2030	129	1	1	531	165 165	0
1-2100	125	1	1	341	151 947	0
1-2130	125	1	1	372	145 180	0
1-2200	147	2	1	337	128 844	0
1-2230	113	1	1	349	123 922	0
1-2300	111	1	1	354	111 405	0
1-2330	120	1	1	331	107 219	0

Instance	Runtime	SS	SS+FD	Energy	Imbalance	Alg-Iter
2-0000	144	2	1	337	100 277	0
2-0030	121	1	1	366	95 590	0
2-0100	122	1	1	333	86 713	0
2-0130	121	1	1	343	82 613	0
2-0200	131	2	1	345	75 110	0
2-0230	137	1	1	388	72 474	0
2-0300	134	1	1	371	61 382	0
2-0330	113	1	1	409	55 359	0
2-0400	134	2	1	304	42 953	0
2-0430	110	1	1	342	35 974	0
2-0500	123	1	1	345	18 148	0
2-0530	114	1	1	323	14 731	0
2-0600	124	2	1	328	9829	0
2-0630	106	1	1	321	11 145	0
2-0700	105	0	0	331	23 023	0
2-0730	120	1	1	314	28 744	0
2-0800	98	0	0	314	40 858	0
2-0830	97	0	0	323	48 902	0
2-0900	125	0	0	281	53 690	0
2-0930	103	0	0	298	58 241	0
2-1000	94	0	0	308	76 918	0
2-1030	102	0	0	271	76 876	0
2-1100	97	0	0	280	74 826	0
2-1130	90	0	0	295	73 034	0
2-1200	99	0	0	286	75 426	0
2-1230	99	0	0	276	75 442	0
2-1300	99	0	0	258	81 898	0
2-1330	112	0	0	260	78 961	0
2-1400	111	0	0	258	82 074	0
2-1430	104	0	0	278	82 156	0
2-1500	103	0	0	261	85 850	0
2-1530	122	0	0	259	82 877	0
2-1600	96	0	0	268	79 443	0
2-1630	95	0	0	288	81 775	0
2-1700	116	0	0	269	86 196	0
2-1730	105	0	0	232	85 050	0
2-1800	96	0	0	262	54 282	0
2-1830	163	1	1	262	42 205	0
2-1900	139	0	0	250	27 585	0
2-1930	99	0	0	261	22 721	0
2-2000	175	1	1	222	16 552	0
2-2030	142	1	1	230	13 716	0
2-2100	141	1	1	228	3134	0
2-2130	262	1	1	237	−1846	0
2-2200	138	1	1	219	−12 776	0
2-2230	364	1	1	235	−17 829	0
2-2300	165	1	1	230	−34 301	0
2-2330	160	1	1	243	−38 623	0

Instance	Runtime	SS	SS+FD	Energy	Imbalance	Alg-Iter
3-0000	189	1	1	265	−48 280	0
3-0030	238	1	1	255	−49 430	0
3-0100	154	1	1	267	−53 977	0
3-0130	176	1	1	252	−56 094	0
3-0200	165	1	1	252	−60 903	0
3-0230	331	1	1	272	−62 536	0
3-0300	164	1	1	260	−62 352	0
3-0330	494	1	1	290	−62 384	0
3-0400	192	1	1	294	−62 547	0
3-0430	146	1	1	256	−63 529	0
3-0500	172	1	1	276	−66 297	0
3-0530	176	1	1	255	−67 443	0
3-0600	261	1	1	259	−72 326	0
3-0630	299	1	1	258	−74 997	0
3-0700	181	1	1	267	−91 772	0
3-0730	560	1	1	275	−102 661	0
3-0800	4081	2	2	239	−119 647	0
3-0830	4141	2	2	239	−119 647	0
3-0900	126	0	0	271	−140 902	0
3-0930	125	0	0	288	−144 744	0
3-1000	164	2	2	262	−122 668	0
3-1030	134	1	1	274	−107 113	0
3-1100	111	0	0	298	−94 310	0
3-1130	115	0	0	234	−83 026	0
3-1200	1153	2	2	264	−62 984	0
3-1230	111	0	0	235	−46 161	0
3-1300	104	0	0	232	−32 108	0
3-1330	106	0	0	223	−23 330	0
3-1400	810	2	2	249	−19 102	0
3-1430	111	0	0	232	−12 246	0
3-1500	113	0	0	230	−1817	0
3-1530	109	0	0	234	3407	0
3-1600	467	2	2	246	8056	0
3-1630	113	0	0	240	8509	0
3-1700	105	0	0	225	11 693	0
3-1730	109	0	0	218	16 959	0
3-1800	668	2	2	222	48 355	0
3-1830	111	0	0	213	64 283	0
3-1900	107	0	0	198	79 035	0
3-1930	103	0	0	204	86 872	0
3-2000	1849	2	2	202	95 943	0
3-2030	112	0	0	284	104 983	0
3-2100	118	1	0	280	120 646	0
3-2130	119	1	1	258	127 026	0
3-2200	797	2	2	236	141 850	0
3-2230	118	0	0	241	152 188	0
3-2300	99	0	0	291	172 286	0
3-2330	112	0	0	255	178 028	0

Instance	Runtime	Slack	SS	SS+FD	Energy	Imbalance	Alg-Iter
4-0000	367	0	1	1	231	191 179	0
4-0030	119	0	0	0	229	189 287	0
4-0100	119	0	0	0	216	187 668	0
4-0130	124	0	0	0	214	184 249	0
4-0200	228	1299	1	1	225	180 193	0
4-0230	112	0	0	0	234	174 014	0
4-0300	107	0	0	0	226	168 700	0
4-0330	107	0	0	0	228	165 410	0
4-0400	235	0	1	1	199	164 319	0
4-0430	107	0	0	0	243	164 428	0
4-0500	117	0	0	0	230	163 655	0
4-0530	124	0	0	0	206	156 890	0
4-0600	101	0	0	0	229	148 258	0
4-0630	107	0	0	0	239	149 214	0
4-0700	127	0	0	0	213	170 571	0
4-0730	131	0	0	0	212	177 632	0
4-0800	124	0	0	0	216	184 110	0
4-0830	112	0	0	0	219	176 705	0
4-0900	108	0	0	0	240	153 710	0
4-0930	148	0	0	0	203	128 466	0
4-1000	107	0	0	0	231	69 704	0
4-1030	109	0	0	0	236	36 310	0
4-1100	114	0	0	0	250	−5012	0
4-1130	114	0	0	0	242	−33 243	0
4-1200	141	0	0	0	239	−80 390	0
4-1230	118	0	0	0	269	−116 126	0
4-1300	113	0	0	0	266	−159 546	0
4-1330	118	0	0	0	276	−184 847	0
4-1400	123	0	0	0	287	−210 481	0
4-1430	123	0	0	0	287	−227 879	0
4-1500	119	0	0	0	286	−253 014	0
4-1530	120	0	0	0	310	−261 979	0
4-1600	142	0	0	0	293	−273 584	0
4-1630	135	0	0	0	286	−280 975	0
4-1700	134	0	0	0	295	−299 741	0
4-1730	146	0	0	0	295	−316 893	0
4-1800	118	0	0	0	333	−332 034	0
4-1830	138	0	0	0	305	−339 961	0
4-1900	138	0	0	0	309	−349 435	0
4-1930	122	0	0	0	362	−353 749	0
4-2000	121	0	0	0	349	−356 692	0
4-2030	129	0	0	0	346	−359 025	0
4-2100	134	0	0	0	323	−358 917	0
4-2130	117	0	0	0	388	−355 127	0
4-2200	136	0	0	0	352	−353 558	0
4-2230	110	0	0	0	382	−350 585	0
4-2300	136	0	0	0	349	−348 497	0
4-2330	139	0	0	0	363	−346 338	0

Instance	Runtime	SS	SS+FD	Energy	Imbalance	Alg-Iter
6-0000	153	1	1	305	−47 740	0
6-0030	196	0	0	316	−43 946	0
6-0100	140	0	0	324	−43 946	0
6-0130	781	1	1	296	−33 954	0
6-0200	162	1	1	299	−33 954	0
6-0230	180	0	0	293	−1546	0
6-0300	142	0	0	315	−1546	0
6-0330	1434	1	1	289	22 146	0
6-0400	1428	1	1	295	22 146	0
6-0430	168	0	0	312	17 257	0
6-0500	188	0	0	306	17 257	0
6-0530	165	1	1	310	22 025	0
6-0600	172	1	1	310	22 025	0
6-0630	158	0	0	296	17 713	0
6-0700	141	0	0	314	25 457	0
6-0730	158	1	1	307	46 146	0
6-0800	359	1	0	282	46 146	0
6-0830	116	0	0	297	62 259	0
6-0900	136	0	0	307	62 259	0
6-0930	153	1	1	285	85 646	0
6-1000	152	1	1	291	85 646	0
6-1030	120	0	0	307	86 849	0
6-1100	135	0	0	306	86 849	0
6-1130	157	1	0	279	80 803	0
6-1200	160	0	0	262	72 775	0
6-1230	208	0	0	273	67 924	0
6-1300	148	0	0	259	61 893	0
6-1330	202	0	0	259	54 410	0
6-1400	268	0	0	268	42 333	0
6-1430	248	0	0	248	34 753	0
6-1500	196	0	0	263	42 136	0
6-1530	620	0	0	256	61 309	0
6-1600	148	0	0	258	92 934	0
6-1630	140	0	0	287	112 419	0
6-1700	125	0	0	276	135 988	0
6-1730	134	0	0	282	149 777	0
6-1800	122	0	0	286	173 170	0
6-1830	141	1	0	260	181 559	0
6-1900	140	1	0	250	192 243	0
6-1930	174	1	0	209	191 720	0
6-2000	162	1	0	219	189 759	0
6-2030	165	1	0	240	194 229	0
6-2100	162	1	0	245	200 822	0
6-2130	463	2	0	263	208 609	0
6-2200	2336	2	0	270	221 339	0
6-2230	157	1	0	291	225 661	0
6-2300	127	1	0	268	231 221	0
6-2330	136	1	0	273	231 616	0

Instance	Runtime	SS	SS+FD	Energy	Imbalance	Alg-Iter
7-0000	110	0	0	297	228 524	0
7-0030	97	0	0	305	220 801	0
7-0100	105	0	0	293	206 007	0
7-0130	107	0	0	290	197 131	0
7-0200	117	0	0	297	184 488	0
7-0230	197	0	0	307	177 394	0
7-0300	136	0	0	296	167 316	0
7-0330	128	0	0	304	162 370	0
7-0400	132	0	0	305	159 063	0
7-0430	113	0	0	315	165 449	0
7-0500	131	0	0	308	177 422	0
7-0530	124	0	0	320	179 615	0
7-0600	128	0	0	325	183 753	0
7-0630	116	0	0	311	181 551	0
7-0700	123	0	0	311	176 015	0
7-0730	122	0	0	324	174 156	0
7-0800	120	0	0	321	172 492	0
7-0830	121	0	0	316	170 943	0
7-0900	117	0	0	302	171 656	0
7-0930	123	0	0	332	167 284	0
7-1000	118	0	0	303	166 693	0
7-1030	121	0	0	306	179 497	0
7-1100	120	0	0	308	195 345	0
7-1130	114	0	0	302	203 253	0
7-1200	121	0	0	326	214 524	0
7-1230	115	0	0	288	215 325	0
7-1300	133	0	0	276	215 108	0
7-1330	124	0	0	277	217 380	0
7-1400	129	0	0	273	212 525	0
7-1430	124	0	0	284	212 613	0
7-1500	113	0	0	305	207 426	0
7-1530	134	0	0	249	203 663	0
7-1600	140	0	0	271	188 892	0
7-1630	131	0	0	290	180 676	0
7-1700	124	0	0	279	171 180	0
7-1730	123	0	0	286	168 865	0
7-1800	134	0	0	269	165 243	0
7-1830	134	0	0	272	160 003	0
7-1900	155	0	0	271	151 932	0
7-1930	122	0	0	271	147 728	0
7-2000	125	0	0	268	140 529	0
7-2030	144	0	0	271	138 114	0
7-2100	128	0	0	266	136 810	0
7-2130	113	0	0	272	136 668	0
7-2200	134	0	0	276	137 491	0
7-2230	107	0	0	281	138 798	0
7-2300	146	0	0	282	140 389	0
7-2330	112	0	0	272	141 463	0

Instance	Runtime	SS	SS+FD	Energy	Imbalance	Alg-Iter
8-0000	128	0	0	288	143 412	0
8-0030	129	0	0	272	147 706	0
8-0100	105	0	0	273	162 764	0
8-0130	105	0	0	285	170 023	0
8-0200	100	0	0	305	177 398	0
8-0230	96	0	0	310	182 791	0
8-0300	106	0	0	291	192 962	0
8-0330	99	0	0	286	195 336	0
8-0400	94	0	0	277	192 778	0
8-0430	100	0	0	276	190 254	0
8-0500	116	0	0	288	187 001	0
8-0530	93	0	0	292	186 046	0
8-0600	119	0	0	268	184 540	0
8-0630	109	0	0	277	184 195	0
8-0700	109	0	0	279	196 707	0
8-0730	109	0	0	276	202 093	0
8-0800	120	0	0	273	209 292	0
8-0830	116	0	0	271	213 198	0
8-0900	115	0	0	267	218 061	0
8-0930	118	0	0	287	224 723	0
8-1000	114	0	0	283	233 656	0
8-1030	147	0	0	258	238 750	0
8-1100	128	0	0	261	257 563	0
8-1130	123	0	0	267	282 241	0
8-1200	131	0	0	273	324 816	0
8-1230	135	0	0	278	358 860	0
8-1300	153	0	0	258	405 887	0
8-1330	113	0	0	278	426 934	0
8-1400	135	0	0	259	459 974	0
8-1430	128	0	0	265	475 915	0
8-1500	120	0	0	267	497 880	0
8-1530	156	0	0	254	511 877	0
8-1600	145	0	0	256	537 500	0
8-1630	135	0	0	260	551 752	0
8-1700	116	0	0	223	566 743	0
8-1730	105	0	0	252	569 700	0
8-1800	114	0	0	238	572 070	0
8-1830	133	0	0	239	572 059	0
8-1900	130	0	0	236	572 307	0
8-1930	109	0	0	288	569 785	0
8-2000	121	0	0	281	567 156	0
8-2030	135	0	0	282	561 602	0
8-2100	114	0	0	259	550 431	0
8-2130	121	0	0	262	543 224	0
8-2200	126	0	0	274	534 997	0
8-2230	150	0	0	264	524 445	0
8-2300	153	0	0	225	505 467	0
8-2330	120	0	0	246	494 317	0

Instance	Runtime	SS	SS+FD	Energy	Imbalance	Alg-Iter
9-0000	121	0	0	251	481 847	0
9-0030	144	0	0	256	479 754	0
9-0100	134	0	0	254	472 289	0
9-0130	149	0	0	230	471 986	0
9-0200	165	0	0	241	473 695	0
9-0230	137	0	0	243	468 894	0
9-0300	123	0	0	209	458 252	0
9-0330	130	0	0	211	453 971	0
9-0400	148	0	0	222	450 731	0
9-0430	129	0	0	228	446 778	0
9-0500	128	0	0	212	439 101	0
9-0530	138	0	0	217	436 740	0
9-0600	138	0	0	208	432 035	0
9-0630	125	0	0	197	427 060	0
9-0700	136	0	0	211	419 863	0
9-0730	118	0	0	188	411 934	0
9-0800	127	0	0	211	401 090	0
9-0830	130	0	0	196	394 350	0
9-0900	130	0	0	202	384 087	0
9-0930	127	0	0	195	373 408	0
9-1000	127	0	0	188	354 511	0

Results for test set H2-12

The columns of the following tables contain the results of the computational experiments for test set H2-12 described and discussed in Section 4. Here, the first column contains the instance name. It consists of the virtual day together with the time in hours and minutes of the corresponding initial state, i.e., 2-0400 is the instance having the initial state from 4am of virtual day 2. The second column denotes the optimality gap for the last solve of a MILP during the tri-level MILP model solve. The third column states the run time of the complete algorithmic approach Algorithm 2 for the corresponding instance until it was terminated. In the fourth column, the total absolute slack used in this instance in kg is given. While the fifth column denotes the total number of conducted simple state changes, the sixth column accounts only for those in which a flow direction change was performed simultaneously. Next, the seventh column states the amount of compression energy that was used in MWh. While the eighth column denotes the flow imbalance in kg, the ninth denotes the maximum difference in the absolute velocity after the last performed IVAP iteration. Finally, the last column states the number of iterations of Algorithm 2, which is equivalent to the number of added no-good-cuts.

Instance	Gap	Runtime	Slack	SS	SS+FD	Energy	Imbalance	Velo	Alg-Iter
1-1200	0	12 985	0	2	1	826	196 221	0.01	0
1-1230	0	123	0	1	1	632	200 803	0.01	0
1-1300	0	148	0	2	1	621	228 390	0.01	0
1-1330	0	147	0	2	1	641	259 195	0.01	0
1-1400	0	138	0	2	1	802	271 807	0.01	0
1-1430	0	139	0	2	1	607	274 882	0.01	0
1-1500	0	127	0	1	1	603	295 830	0.01	0
1-1530	0	204	0	2	1	648	299 909	0.01	0
1-1600	0	174	0	2	1	638	313 968	0.01	0
1-1630	0	300	0	2	1	799	318 467	0.01	0
1-1700	0	3099	0	2	1	781	309 042	0.01	0
1-1730	0	138	0	2	1	654	303 524	0.01	0
1-1800	0	136	0	2	1	755	290 122	0.01	0
1-1830	0	158	0	2	1	558	284 693	0.01	0
1-1900	0	164	0	2	1	544	269 038	0.01	0
1-1930	0	139	0	2	1	574	261 650	0.01	0
1-2000	0	192	1191	2	1	493	239 274	0.01	0
1-2030	0	147	0	2	1	543	227 371	0.01	0
1-2100	0	136	0	2	1	733	204 314	0.01	0
1-2130	0	137	0	2	1	518	194 252	0.01	0
1-2200	0	166	1191	2	1	517	169 936	0.01	0
1-2230	0	135	0	2	1	498	162 252	0.01	0
1-2300	0	139	0	2	1	625	141 328	0.01	0
1-2330	0	146	0	2	1	485	134 800	0.01	0

Instance	Gap	Runtime	Slack	SS	SS+FD	Energy	Imbalance	Velo	Alg-Iter
2-0000	0	179	1191	2	1	519	125 941	0.01	0
2-0030	0	132	0	2	1	490	119 837	0.01	0
2-0100	0	757	0	2	1	505	105 596	0.01	0
2-0130	0	888	0	2	1	829	99 833	0.01	0
2-0200	0	178	1840	2	1	512	91 659	0.01	0
2-0230	0	2188	0	2	1	731	89 301	0.01	0
2-0300	0	4240	0	2	1	514	73 764	0.01	0
2-0330	0	2549	0	2	1	717	65 491	0.01	0
2-0400	0	291	1692	2	1	495	50 783	0.01	0
2-0430	0	4181	0	2	1	696	42 786	0.01	0
2-0500	0	10 291	0	2	1	503	20 212	0.01	0
2-0530	0	4681	0	2	1	583	15 275	0.01	0
2-0600	0	265	10 258	1	1	670	11 130	0.01	0
2-0630	0	7843	0	2	1	459	12 551	0.01	0
2-0700	0	4162	0	2	2	668	29 456	0.01	0
2-0730	0	368	0	2	2	700	37 857	0.01	0
2-0800	0	333	4986	2	1	707	54 379	0.01	0
2-0830	0	786	0	2	2	702	65 519	0.01	0
2-0900	0	298	0	2	2	622	76 787	0.01	0
2-0930	0	160	0	2	2	601	83 398	0.01	0
2-1000	0	198	6522	1	1	575	105 309	0.01	0
2-1030	0	245	0	2	2	529	105 550	0.01	0
2-1100	0	250	0	2	2	567	109 497	0.01	0
2-1130	0	211	0	2	2	476	108 373	0.01	0
2-1200	0	197	11 221	1	1	528	112 657	0.01	0
2-1230	0	1861	0	2	2	493	112 616	0.01	0
2-1300	0	253	0	2	2	483	125 616	0.01	0
2-1330	0	447	0	2	2	510	124 327	0.01	0
2-1400	0	213	1608	2	2	505	134 552	0.01	0
2-1430	0	176	0	2	2	473	136 292	0.01	0
2-1500	0	425	0	2	2	446	143 887	0.01	0
2-1530	0	171	0	2	2	506	140 771	0.01	0
2-1600	0	262	1859	2	2	508	138 487	0.01	0
2-1630	0	280	0	2	2	473	141 867	0.01	0
2-1700	0	252	0	2	2	428	147 674	0.01	0
2-1730	0	224	0	2	2	446	145 457	0.01	0
2-1800	0	355	1946	2	2	434	96 897	0.01	0
2-1830	0	192	0	2	2	441	78 404	0.01	0
2-1900	0	303	3730	2	2	409	56 327	0.01	0
2-1930	0	211	0	2	2	415	48 333	0.01	0
2-2000	0	236	0	2	2	406	35 540	0.01	0
2-2030	0	155	0	2	2	410	28 486	0.01	0
2-2100	0	175	0	2	2	412	7801	0.01	0
2-2130	0	170	0	2	2	387	−1459	0.01	0
2-2200	0	179	0	2	2	404	−22 755	0.01	0
2-2230	0	162	0	2	2	483	−32 629	0.01	0
2-2300	0	154	0	2	2	397	−63 624	0.01	0
2-2330	0	209	0	2	1	480	−71 813	0.01	0

Instance	Gap	Runtime	Slack	SS	SS+FD	Energy	Imbalance	Velo	Alg-Iter
3-0000	0	165	0	2	2	362	−88 313	0.01	0
3-0030	0	162	0	2	2	512	−91 007	0.01	0
3-0100	0	219	0	2	2	379	−100 904	0.01	0
3-0130	0	276	0	2	2	363	−105 272	0.01	0
3-0200	0	154	0	2	2	469	−113 407	0.01	0
3-0230	0	160	0	2	2	546	−115 464	0.01	0
3-0300	0	624	0	2	2	368	−117 654	0.01	0
3-0330	0	203	0	2	2	410	−119 037	0.01	0
3-0400	0	184	0	2	2	582	−121 706	0.01	0
3-0430	0	182	0	2	1	405	−124 473	0.01	0
3-0500	0	183	0	2	2	377	−133 590	0.01	0
3-0530	0	371	0	2	2	403	−137 212	0.01	0
3-0600	0	187	0	2	2	601	−147 452	0.01	0
3-0630	0	182	0	2	2	390	−151 782	0.01	0
3-0700	0	194	0	2	2	475	−178 420	0.01	0
3-0730	0	160	0	2	2	573	−193 955	0.01	0
3-0800	0	164	76 635	1	1	470	−217 307	0.01	0
3-0830	0	165	76 635	1	1	470	−217 307	0.01	0
3-0900	0	164	0	2	2	455	−243 740	0.01	0
3-0930	0	182	0	2	2	638	−246 032	0.01	0
3-1000	0	137	66 879	1	1	578	−207 073	0.01	0
3-1030	0	156	0	2	2	456	−179 862	0.01	0
3-1100	0	169	0	2	2	500	−153 250	0.01	0
3-1130	0	122	5709	1	1	385	−132 333	0.01	0
3-1200	0	204	65 125	1	1	579	−95 675	0.01	0
3-1230	0	124	6639	1	1	429	−66 602	0.01	0
3-1300	0	118	1912	1	1	455	−35 922	0.01	0
3-1330	0	113	2144	1	1	399	−17 193	0.01	0
3-1400	0	127	68 960	1	1	385	47	0.01	0
3-1430	0	125	1245	1	1	380	15 600	0.01	0
3-1500	0	121	1515	1	1	381	38 656	0.01	0
3-1530	0	116	2615	1	1	428	48 860	0.01	0
3-1600	0	141	62 556	1	1	395	62 291	0.01	0
3-1630	0	123	1293	1	1	377	67 102	0.01	0
3-1700	0	198	1558	1	1	405	78 536	0.01	0
3-1730	0	130	2173	1	1	459	88 576	0.01	0
3-1800	0	135	57 659	1	1	445	127 115	0.01	0
3-1830	0	122	2017	1	1	370	147 900	0.01	0
3-1900	0	123	1690	1	1	358	169 485	0.01	0
3-1930	0	127	2501	1	1	352	180 132	0.01	0
3-2000	0	123	74 890	1	1	352	192 433	0.01	0
3-2030	0	174	2570	1	1	485	203 542	0.01	0
3-2100	0	205	1390	2	1	583	224 485	0.01	0
3-2130	0	135	1715	2	2	502	232 206	0.01	0
3-2200	0	202	51 283	2	2	470	251 568	0.01	0
3-2230	0	142	1958	1	1	417	264 044	0.01	0
3-2300	0	175	906	1	1	420	288 222	0.01	0
3-2330	0	117	2231	1	1	421	295 015	0.01	0

Instance	Gap	Runtime	Slack	SS	SS+FD	Energy	Imbalance	Velo	Alg-Iter
4-0000	0	169	41 574	1	1	470	311 397	0.01	0
4-0030	0	152	1123	1	1	397	306 696	0.01	0
4-0100	0	140	917	1	1	371	301 619	0.01	0
4-0130	0	125	1796	1	1	400	294 360	0.01	0
4-0200	0	133	31 483	1	1	361	283 582	0.01	0
4-0230	0	144	2689	1	1	419	271 824	0.01	0
4-0300	0	159	1900	1	1	318	261 349	0.01	0
4-0330	0	151	2723	1	1	465	254 399	0.01	0
4-0400	0	135	28 882	1	1	382	248 388	0.01	0
4-0430	0	134	2153	1	1	310	244 084	0.01	0
4-0500	0	151	2492	1	1	469	236 946	0.01	0
4-0530	0	163	3194	1	1	363	222 741	0.01	0
4-0600	0	150	2690	1	1	374	202 882	0.01	0
4-0630	0	160	2390	1	1	271	200 742	0.01	0
4-0700	0	149	3580	1	1	352	226 213	0.01	0
4-0730	0	215	3935	1	1	481	230 809	0.01	0
4-0800	0	145	3300	1	1	381	231 608	0.01	0
4-0830	0	152	4243	1	1	445	214 554	0.01	0
4-0900	0	169	3490	1	1	348	168 589	0.01	0
4-0930	0	178	3883	1	1	345	125 462	0.01	0
4-1000	0	227	4390	1	1	354	39 724	0.01	0
4-1030	0	202	4928	1	1	497	−8538	0.01	0
4-1100	0	142	4136	1	1	364	−68 753	0.01	0
4-1130	0	129	3829	1	1	401	−109 469	0.01	0
4-1200	0	148	3923	1	1	516	−176 742	0.01	0
4-1230	0	157	4323	1	1	611	−227 424	0.01	0
4-1300	0	161	3514	1	1	702	−287 268	0.01	0
4-1330	0	168	3342	1	1	733	−321 801	0.01	0
4-1400	0	310	5592	1	1	817	−357 295	0.01	0
4-1430	0	277	4999	1	1	655	−380 060	0.01	0
4-1500	0	198	3757	1	1	810	−413 426	0.01	0
4-1530	0	155	3107	2	1	635	−424 504	0.01	0
4-1600	0	163	3907	1	1	786	−440 844	0.01	0
4-1630	0	422	4582	1	1	899	−450 859	0.01	0
4-1700	0	182	3311	1	1	1012	−479 099	0.01	0
4-1730	0	289	3670	2	2	721	−504 551	0.01	0
4-1800	0	306	4320	1	1	806	−528 032	0.01	0
4-1830	0	186	5108	1	1	894	−539 093	0.01	0
4-1900	0	191	3427	1	1	1062	−551 767	0.01	0
4-1930	0	188	3175	2	2	847	−556 988	0.01	0
4-2000	0	171	3245	1	1	1218	−561 721	0.01	0
4-2030	0	191	3216	1	1	1129	−565 503	0.01	0
4-2100	0	358	3551	1	1	1160	−564 999	0.01	0
4-2130	0	246	3362	2	2	864	−558 911	0.01	0
4-2200	0	303	3886	2	1	910	−555 405	0.01	0
4-2230	0	187	3676	1	1	1256	−548 955	0.01	0
4-2300	0	345	3291	2	1	1092	−543 000	0.01	0
4-2330	0	327	2832	2	1	1075	−536 270	0.01	0

Instance	Gap	Runtime	Slack	SS	SS+FD	Energy	Imbalance	Velo	Alg-Iter
6-0000	0	5092	0	3	2	485	−81 561	0.01	0
6-0030	0	4850	0	3	1	468	−66 951	0.01	0
6-0100	0	7447	0	3	2	462	−66 980	0.01	0
6-0130	0	19 150	0	3	1	494	−48 479	0.01	0
6-0200	0	8047	0	3	2	460	−48 499	0.01	0
6-0230	0	7291	0	3	2	496	−1362	0.01	0
6-0300	0	11 342	0	3	1	476	−1362	0.01	0
6-0330	0	7862	0	3	1	473	34 176	0.01	0
6-0400	0	12 745	0	3	2	491	34 175	0.01	0
6-0430	0	7726	0	3	1	464	32 144	0.01	0
6-0500	0	26 191	0	3	1	532	32 151	0.01	0
6-0530	0	63 309	0	3	2	489	45 863	0.01	0
6-0600	0	28 566	0	3	1	461	45 847	0.01	0
6-0630	0	31 765	0	3	0	457	47 291	0.01	0
6-0700	0.13	86 583	0	2	2	846	59 739	0.01	0
6-0730	0.05	86 577	0	2	0	741	93 618	0.01	0
6-0800	0	396	0	2	1	658	93 571	0.01	0
6-0830	0	154	0	2	2	698	120 340	0.01	0
6-0900	0	49 668	0	3	1	761	120 312	0.01	0
6-0930	0.24	86 556	0	3	2	532	159 513	0.01	0
6-1000	0	64 827	0	3	2	659	159 484	0.01	0
6-1030	0	44 144	0	3	1	843	157 978	13.70	150
6-1100	0	2209	0	3	1	504	157 948	0.01	1
6-1130	0	22 480	0	3	2	673	149 431	0.01	0
6-1200	0	236	0	2	1	757	139 040	0.01	1
6-1230	0	232	0	2	1	831	132 215	0.01	0
6-1300	0	167	0	1	1	707	123 504	0.01	0
6-1330	0	27 363	0	2	1	597	114 878	0.01	0
6-1400	0	55 973	0	2	0	608	103 478	0.01	0
6-1430	0	38 837	0	2	0	641	96 375	0.01	0
6-1500	0	2442	0	2	1	379	105 879	0.01	0
6-1530	0	176	0	1	0	480	126 626	0.01	0
6-1600	0	640	0	2	1	430	161 323	0.01	0
6-1630	0	3870	0	2	0	424	181 205	0.01	0
6-1700	0	542	0	2	0	454	204 770	0.01	0
6-1730	0	166	0	2	1	639	218 367	0.01	0
6-1800	0	297	0	2	1	612	243 059	0.01	0
6-1830	0	605	0	3	1	774	253 805	0.01	0
6-1900	0.08	86 553	0	3	0	653	268 247	0.01	0
6-1930	0	1300	0	3	0	424	270 204	0.01	0
6-2000	0.05	86 694	0	3	0	414	272 231	0.01	0
6-2030	0	3688	0	3	0	732	279 046	0.01	0
6-2100	0	81 009	0	3	1	488	289 418	0.01	0
6-2130	0	575	0	3	1	820	299 280	0.01	0
6-2200	0	250	0	3	1	860	314 477	0.01	0
6-2230	0.09	86 573	0	3	0	626	320 576	0.01	0
6-2300	0	45 056	0	3	1	557	329 160	0.01	0
6-2330	0.30	86 589	0	3	0	855	330 600	0.01	0

Instance	Gap	Runtime	Slack	SS	SS+FD	Energy	Imbalance	Velo	Alg-Iter
7-0000	0	4435	0	2	0	527	327 208	0.01	0
7-0030	0	367	0	2	0	497	317 284	0.01	0
7-0100	0	11 020	0	2	1	489	296 723	0.01	0
7-0130	0	749	0	2	1	488	282 240	0.01	0
7-0200	0	6768	0	2	1	568	262 057	0.01	0
7-0230	0	170	0	2	1	641	254 259	0.01	0
7-0300	0	225	0	2	0	462	244 234	0.01	0
7-0330	0	284	0	2	0	456	240 134	0.01	0
7-0400	0	261	0	2	1	465	239 965	0.01	0
7-0430	0	337	0	2	1	463	251 175	0.01	0
7-0500	0	308	0	2	1	457	271 359	0.01	0
7-0530	0	215	0	2	1	523	276 113	0.01	0
7-0600	0	204	0	2	0	505	284 517	0.01	0
7-0630	0	203	0	2	1	467	281 870	0.01	0
7-0700	0	244	0	2	1	508	276 206	0.01	0
7-0730	0	223	0	2	0	469	275 177	0.01	0
7-0800	0	225	0	2	1	464	274 127	0.01	0
7-0830	0	402	0	2	0	490	273 161	0.01	0
7-0900	0	197	0	2	0	478	275 673	0.01	0
7-0930	0	198	0	2	0	434	273 064	0.01	0
7-1000	0	990	0	2	0	500	277 111	0.01	0
7-1030	0	237	0	2	0	508	295 430	0.01	0
7-1100	0	210	0	2	0	494	316 135	0.01	0
7-1130	0	162	0	2	1	673	324 483	0.01	0
7-1200	0	157	0	2	0	808	336 551	0.01	0
7-1230	0	169	0	2	1	878	334 411	0.01	0
7-1300	0	200	0	2	0	617	328 442	0.01	0
7-1330	0	85 215	0	2	0	651	328 522	0.01	0
7-1400	0	4081	0	2	1	603	316 557	0.01	0
7-1430	0	161	0	2	1	685	313 886	0.01	0
7-1500	0	247	0	2	0	446	301 512	0.01	0
7-1530	0	201	0	2	0	449	292 792	0.01	0
7-1600	0	221	0	2	0	429	265 942	0.01	0
7-1630	0	262	0	2	0	430	250 105	0.01	0
7-1700	0	211	0	2	0	430	230 927	0.01	0
7-1730	0	2076	0	2	0	462	225 575	0.01	0
7-1800	0	373	0	2	0	453	218 899	0.01	0
7-1830	0	252	0	2	0	405	212 091	0.01	0
7-1900	0	301	0	2	1	460	202 170	0.01	0
7-1930	0	1461	0	2	0	507	197 770	0.01	0
7-2000	0	299	0	2	0	483	189 978	0.01	0
7-2030	0	292	0	2	0	635	187 910	0.01	0
7-2100	0	294	0	2	0	505	189 173	0.01	0
7-2130	0	1229	0	2	1	476	191 104	0.01	0
7-2200	0	1047	0	2	0	462	194 699	0.01	0
7-2230	0	454	0	2	1	497	199 168	0.01	0
7-2300	0	267	0	2	0	523	206 098	0.01	0
7-2330	0	181	0	2	1	435	211 121	0.01	0

Instance	Gap	Runtime	Slack	SS	SS+FD	Energy	Imbalance	Velo	Alg-Iter
8-0000	0	623	0	2	0	480	216 767	0.01	0
8-0030	0	161	0	2	1	732	222 033	0.01	0
8-0100	0	174	0	2	1	663	241 713	0.01	0
8-0130	0	184	0	2	1	734	249 201	0.01	0
8-0200	0	159	0	2	1	596	254 695	0.01	0
8-0230	0	4002	0	2	1	407	262 161	0.01	0
8-0300	0	139	0	1	1	781	277 618	0.01	0
8-0330	0	137	0	1	1	706	281 627	0.01	0
8-0400	0	128	0	1	1	479	279 231	0.01	0
8-0430	0	162	0	1	1	510	278 419	0.01	0
8-0500	0	145	0	1	1	459	279 546	0.01	0
8-0530	0	142	0	1	1	452	280 502	0.01	0
8-0600	0	163	0	1	1	477	283 337	0.01	0
8-0630	0	163	0	1	1	448	282 383	0.01	0
8-0700	0	179	0	1	1	465	302 682	0.01	0
8-0730	0	168	0	1	1	451	312 270	0.01	0
8-0800	0	176	0	1	1	460	325 435	0.01	0
8-0830	0	162	0	1	1	453	332 651	0.01	0
8-0900	0	150	0	1	1	523	342 768	0.01	0
8-0930	0	144	0	1	1	393	354 440	0.01	0
8-1000	0	187	0	1	1	393	373 587	0.01	0
8-1030	0	1935	0	2	0	426	386 853	0.01	0
8-1100	0	4029	0	1	0	542	421 392	0.01	0
8-1130	0	1824	0	1	1	608	461 205	0.01	0
8-1200	0	147	0	1	1	734	531 646	0.01	0
8-1230	0	225	0	2	1	523	583 975	0.01	0
8-1300	0	10 537	0	2	2	613	655 687	0.01	0
8-1330	0.31	86 921	0	2	2	553	687 609	0.01	0
8-1400	0	31 255	0	2	1	627	736 300	0.01	0
8-1430	0	25 981	0	2	1	632	760 576	0.01	0
8-1500	0.18	86 611	0	4	1	635	790 235	0.01	0
8-1530	0.40	86 786	0	5	1	557	808 546	0.01	0
8-1600	0.36	86 798	0	3	3	492	839 501	0.01	0
8-1630	0	111 679	0	3	1	502	855 331	0.01	0
8-1700	0.44	86 880	0	4	1	463	869 448	0.01	0
8-1730	0.36	86 688	0	3	3	352	871 503	0.01	0
8-1800	0.31	86 631	0	3	1	354	872 964	0.01	0
8-1830	0.34	86 859	0	3	2	422	871 689	0.01	0
8-1900	0.35	86 557	0	3	2	529	869 706	0.01	0
8-1930	0	11 454	0	2	1	450	865 098	0.01	0
8-2000	0.19	86 587	0	2	1	419	860 523	0.01	0
8-2030	0	701	0	2	2	596	850 871	0.01	0
8-2100	0	985	0	2	2	591	833 006	0.01	0
8-2130	0	5177	0	2	2	549	822 577	0.01	0
8-2200	0	4793	0	2	2	553	810 610	0.01	0
8-2230	0	1927	0	2	1	548	795 510	0.01	0
8-2300	0.17	86 579	0	2	2	533	767 197	0.01	0
8-2330	0	3275	0	2	1	505	750 929	0.01	0

Instance	Gap	Runtime	Slack	SS	SS+FD	Energy	Imbalance	Velo	Alg-Iter
9-0000	0	53 421	0	2	2	510	731 916	0.01	0
9-0030	0	4446	0	2	1	514	727 094	0.01	0
9-0100	0	773	0	2	1	487	714 590	0.01	0
9-0130	0	594	0	2	1	524	709 726	0.01	0
9-0200	0	5125	0	2	2	491	705 648	0.01	0
9-0230	0	2476	0	2	1	493	694 871	0.01	0
9-0300	0	6026	0	2	2	474	675 792	0.01	0
9-0330	0	1429	0	2	2	485	665 780	0.01	0
9-0400	0	217	365	2	1	405	653 514	0.01	0
9-0430	0	242	156	2	1	479	643 702	0.01	0
9-0500	0	1179	7122	1	1	512	627 727	0.01	0
9-0530	0	167	566	1	1	472	619 453	0.01	0
9-0600	0	126	0	1	1	434	605 917	0.01	0
9-0630	0	140	455	1	1	441	593 172	0.01	0
9-0700	0	149	227	1	1	418	576 024	0.01	0
9-0730	0	137	457	1	1	404	560 483	0.01	0
9-0800	0	150	0	1	1	358	538 595	0.01	0
9-0830	0	139	0	1	1	387	524 295	0.01	0
9-0900	0	146	266	1	1	368	503 259	0.01	0
9-0930	0	149	207	1	1	357	485 197	0.01	0
9-1000	0	157	0	1	1	366	454 209	0.01	0

Results for test set H2-34

The columns of the following tables contain the results of the computational experiments for test set H2-34 described and discussed in Section 4. Here, the first column contains the instance name. It consists of the virtual day together with the time in hours and minutes of the corresponding initial state, i.e., 2-0400 is the instance having the initial state from 4am of virtual day 2. The second column denotes the optimality gap for the last solve of a MILP during the tri-level MILP model solve. The third column states the run time of the complete algorithmic approach Algorithm 2 for the corresponding instance until it was terminated. In the fourth column, the total absolute slack used in this instance in kg is given. While the fifth column denotes the total number of conducted simple state changes, the sixth column accounts only for those in which a flow direction change was performed simultaneously. Next, the seventh column states the amount of compression energy that was used in MWh. While the eighth column denotes the flow imbalance in kg, the ninth denotes the maximum difference in the absolute velocity after the last performed IVAP iteration. Finally, the last column states the number of iterations of Algorithm 2, which is equivalent to the number of added no-good-cuts.

Instance	Gap	Runtime	Slack	SS	SS+FD	Energy	Imbalance	Velo	Alg-Iter
1-1200	0	182	0	2	1	1108	313 484	0.01	0
1-1230	0	167	0	1	1	1164	320 402	0.01	0
1-1300	0	182	0	2	1	1223	353 283	0.01	0
1-1330	0	190	0	2	1	1244	391 517	0.01	0
1-1400	0	179	0	2	1	1127	409 364	0.01	0
1-1430	0	186	0	2	1	1158	413 438	0.01	0
1-1500	0	175	0	1	1	1224	436 124	0.01	0
1-1530	0	191	0	2	1	1183	441 061	0.01	0
1-1600	0	178	0	2	1	1135	454 841	0.01	0
1-1630	0	1701	0	2	1	1155	456 690	0.01	0
1-1700	0	182	0	2	1	1179	438 101	0.01	0
1-1730	0	170	0	2	1	1118	428 575	0.01	0
1-1800	0	199	0	2	1	1123	407 593	0.01	0
1-1830	0	185	0	2	1	1117	399 457	0.01	0
1-1900	0	175	0	2	1	1090	375 663	0.01	0
1-1930	0	166	0	2	1	1065	363 911	0.01	0
1-2000	0	268	1785	2	1	1015	329 121	0.01	0
1-2030	0	169	0	2	1	1054	310 562	0.01	0
1-2100	0	1219	0	2	1	972	274 369	0.01	0
1-2130	0	168	0	2	1	1006	259 876	0.01	0
1-2200	0	333	532	2	1	1127	224 886	0.01	0
1-2230	0	169	0	2	1	997	213 513	0.01	0
1-2300	0	169	0	2	1	968	181 342	0.01	0
1-2330	0	168	0	2	1	1014	171 690	0.01	0

Instance	Gap	Runtime	Slack	SS	SS+FD	Energy	Imbalance	Velo	Alg-Iter
2-0000	0	357	1162	2	1	990	160 270	0.01	0
2-0030	0	240	0	2	1	1033	152 265	0.01	0
2-0100	0	171	0	2	1	976	130 847	0.01	0
2-0130	0	206	0	2	1	1006	122 851	0.01	0
2-0200	0	281	1784	2	1	1001	113 781	0.01	0
2-0230	0	169	0	2	1	956	111 790	0.01	0
2-0300	0	173	0	2	1	1068	90 302	0.01	0
2-0330	0	166	0	2	1	958	79 026	0.01	0
2-0400	0	181	7742	2	1	996	61 241	0.01	0
2-0430	0	181	0	3	2	1031	51 883	0.01	0
2-0500	0	183	0	3	2	1042	22 969	0.01	0
2-0530	0	200	0	3	2	962	16 000	0.01	0
2-0600	0	299	6703	2	1	917	12 867	0.01	0
2-0630	0	213	0	3	2	998	14 428	0.01	0
2-0700	0	243	0	3	2	1046	38 049	0.01	0
2-0730	0	1155	0	3	2	969	50 029	0.01	0
2-0800	0	330	1788	3	2	965	72 429	0.01	0
2-0830	0	234	0	3	2	1071	87 711	0.01	0
2-0900	0	222	0	3	2	927	107 641	0.01	0
2-0930	0	239	0	3	2	954	117 033	0.01	0
2-1000	0	756	1255	3	2	1016	143 207	0.01	0
2-1030	0	262	0	3	2	956	143 831	0.01	0
2-1100	0	197	0	3	2	1031	155 802	0.01	0
2-1130	0	311	0	3	2	1038	155 609	0.01	0
2-1200	0	423	1216	3	2	953	162 367	0.01	0
2-1230	0	1114	0	3	2	1117	162 319	0.01	0
2-1300	0	1249	0	3	2	1028	184 094	0.01	0
2-1330	0	612	0	3	2	1096	185 019	0.01	0
2-1400	0	467	1725	3	2	972	204 690	0.01	0
2-1430	0	847	0	3	2	1101	208 654	0.01	0
2-1500	0	194	0	3	2	908	221 457	0.01	0
2-1530	0	394	0	3	2	994	218 179	0.01	0
2-1600	0	815	1944	3	2	927	217 406	0.01	0
2-1630	0	948	0	3	2	879	222 187	0.01	0
2-1700	0	198	0	3	2	831	229 822	0.01	0
2-1730	0	239	0	3	2	844	226 189	0.01	0
2-1800	0	380	1772	3	2	941	153 872	0.01	0
2-1830	0	188	0	3	2	843	126 803	0.01	0
2-1900	0	1152	1662	3	2	887	94 760	0.01	0
2-1930	0	248	0	3	2	894	82 575	0.01	0
2-2000	0	2240	0	3	2	863	60 924	0.01	0
2-2030	0	189	0	3	2	848	48 237	0.01	0
2-2100	0	906	0	3	2	897	14 041	0.01	0
2-2130	0	281	0	3	2	905	−941	0.01	0
2-2200	0	1955	0	3	2	805	−36 104	0.01	0
2-2230	0	845	0	3	2	815	−52 413	0.01	0
2-2300	0	871	0	3	1	877	−102 858	0.01	0
2-2330	0	265	0	3	2	806	−116 226	0.01	0

Instance	Gap	Runtime	Slack	SS	SS+FD	Energy	Imbalance	Velo	Alg-Iter
3-0000	0	369	0	3	2	741	−141 877	0.01	0
3-0030	0	308	0	3	2	854	−146 653	0.01	0
3-0100	0	233	0	3	2	937	−163 611	0.01	0
3-0130	0	669	0	3	2	880	−171 015	0.01	0
3-0200	0	832	0	3	2	683	−183 583	0.01	0
3-0230	0	827	0	3	2	731	−186 180	0.01	0
3-0300	0	1204	0	3	2	758	−191 556	0.01	0
3-0330	0	543	0	3	2	754	−194 733	0.01	0
3-0400	0	743	0	3	1	736	−200 746	0.01	0
3-0430	0	328	0	3	2	714	−205 868	0.01	0
3-0500	0	419	984	3	2	788	−223 465	0.01	0
3-0530	0	479	0	3	2	854	−230 394	0.01	0
3-0600	0	338	0	3	2	751	−247 775	0.01	0
3-0630	0	517	0	3	2	846	−254 284	0.01	0
3-0700	0	429	651	3	2	793	−294 135	0.01	0
3-0730	0	566	0	3	2	769	−315 874	0.01	0
3-0800	0	1237	90 672	3	2	828	−347 721	0.01	0
3-0830	0	1235	90 672	3	2	828	−347 721	0.01	0
3-0900	0	246	12 907	1	1	855	−381 088	0.01	0
3-0930	0	190	0	2	2	960	−381 354	0.01	0
3-1000	0	328	100 014	1	1	1424	−319 730	0.01	0
3-1030	0	202	49 569	1	1	841	−277 036	0.01	1
3-1100	0	218	6058	1	1	1003	−231 972	0.01	0
3-1130	0	218	7096	1	1	998	−198 128	0.01	0
3-1200	0	154	97 773	1	1	736	−139 338	0.01	0
3-1230	0	258	32 038	1	1	838	−93 868	0.01	1
3-1300	0	132	1751	1	1	744	−41 009	0.01	0
3-1330	0	127	3334	1	1	715	−9008	0.01	0
3-1400	0	138	91 281	1	1	743	25 602	0.01	0
3-1430	0	159	29 902	1	1	701	52 803	0.01	1
3-1500	0	133	1462	1	1	806	92 684	0.01	0
3-1530	0	122	3133	1	1	697	109 534	0.01	0
3-1600	0	158	91 448	1	1	852	134 654	0.01	0
3-1630	0	137	18 942	1	1	692	145 293	0.01	1
3-1700	0	123	1577	1	1	711	167 743	0.01	0
3-1730	0	136	3096	1	1	808	184 297	0.01	0
3-1800	0	141	83 246	1	1	809	232 490	0.01	0
3-1830	0	154	17 923	1	1	683	259 666	0.01	1
3-1900	0	137	1732	1	1	772	290 408	0.01	0
3-1930	0	133	2035	1	1	703	304 841	0.01	0
3-2000	0	171	92 715	1	1	743	321 478	0.01	0
3-2030	0	175	26 134	1	1	850	335 374	0.01	1
3-2100	0	186	1303	2	1	857	363 372	0.01	0
3-2130	0	154	1885	2	2	937	372 904	0.01	0
3-2200	0	170	54 520	2	2	883	398 334	0.01	0
3-2230	0	182	4218	1	1	832	413 778	0.01	1
3-2300	0	157	744	1	1	872	443 324	0.01	0
3-2330	0	169	1434	1	1	802	451 396	0.01	1

Instance	Gap	Runtime	Slack	SS	SS+FD	Energy	Imbalance	Velo	Alg-Iter
4-0000	0	184	43 509	1	1	834	472 145	0.01	0
4-0030	0	209	80	1	1	856	463 669	0.01	0
4-0100	0	160	728	1	1	821	453 936	0.01	0
4-0130	0	335	2353	1	1	653	441 455	0.01	2
4-0200	0	242	36 303	1	1	779	421 694	0.01	0
4-0230	0	169	1991	1	1	688	402 473	0.01	0
4-0300	0	12 835	2724	2	1	723	385 079	0.01	141
4-0330	0	188	3469	1	1	698	373 286	0.01	1
4-0400	0	212	34 605	1	1	725	360 663	0.01	0
4-0430	0	264	3149	1	1	690	350 516	0.01	0
4-0500	0	159	3613	1	1	621	334 871	0.01	0
4-0530	0	184	4193	1	1	673	310 761	0.01	1
4-0600	0	172	3582	1	1	587	275 880	0.01	0
4-0630	0	172	3863	1	1	628	269 437	0.01	0
4-0700	0	191	3929	1	1	585	300 418	0.01	0
4-0730	0	253	5494	1	1	669	301 882	0.01	1
4-0800	0	473	4282	1	1	624	295 035	0.01	0
4-0830	0	217	3728	1	1	623	265 090	0.01	0
4-0900	0	247	4470	1	1	713	188 460	0.01	0
4-0930	0	186	5496	1	1	591	121 442	0.01	1
4-1000	0	194	5480	1	1	673	−390	0.01	1
4-1030	0	177	5434	1	1	896	−68 551	0.01	0
4-1100	0	216	4164	1	1	739	−153 820	0.01	0
4-1130	0	2409	4338	1	1	795	−211 184	0.01	3
4-1200	0	174	6108	1	1	949	−305 290	0.01	0
4-1230	0	222	4340	1	1	917	−375 913	0.01	0
4-1300	0	220	3920	1	1	1245	−457 698	0.01	0
4-1330	0	184	4469	1	1	1162	−504 493	0.01	0
4-1400	0	348	5400	1	1	1197	−553 139	0.01	0
4-1430	0	277	5994	1	1	1468	−583 268	0.01	0
4-1500	0	195	4627	1	1	1491	−627 602	0.01	0
4-1530	0	173	4526	2	1	1384	−642 026	0.01	0
4-1600	0	193	4487	1	1	1543	−664 396	0.01	0
4-1630	0	206	4742	1	1	1576	−678 124	0.01	0
4-1700	0	234	3603	1	1	1804	−719 176	0.01	0
4-1730	0	206	4538	2	2	1592	−755 687	0.01	0
4-1800	0	275	4323	1	1	1703	−790 401	0.01	0
4-1830	0	351	5642	1	1	1929	−805 544	0.01	0
4-1900	0	211	4814	1	1	1906	−822 518	0.01	0
4-1930	0	179	4102	2	2	1875	−829 079	0.01	0
4-2000	0	293	7203	1	1	1920	−836 238	0.01	0
4-2030	0	227	5439	1	1	2053	−841 990	0.01	0
4-2100	0	247	5178	1	1	2002	−840 915	0.01	0
4-2130	0	360	9894	2	2	2034	−831 788	0.01	0
4-2200	0	322	5369	2	2	2181	−825 644	0.01	0
4-2230	0	238	6851	1	1	2354	−814 680	0.01	0
4-2300	0	756	6303	2	2	2304	−803 636	0.01	0
4-2330	0	757	4110	2	2	2217	−790 802	0.01	1

Instance	Gap	Runtime	Slack	SS	SS+FD	Energy	Imbalance	Velo	Alg-Iter
6-0000	0	552	0	3	1	1282	−126 726	0.01	0
6-0030	0	245	0	3	2	1312	−97 645	0.01	0
6-0100	0	222	0	3	2	1350	−97 688	0.01	0
6-0130	0	394	0	3	2	1450	−67 871	0.01	0
6-0200	0	631	0	3	1	1616	−67 901	0.01	0
6-0230	0	208	0	3	2	1603	−1117	0.01	0
6-0300	0	211	0	3	2	1512	−1117	0.01	0
6-0330	0	283	0	3	2	1338	50 242	0.01	0
6-0400	0	290	0	3	2	1528	50 241	0.01	0
6-0430	0	223	0	3	2	1244	52 018	0.01	0
6-0500	0	231	0	3	2	1068	52 029	0.01	0
6-0530	0	542	0	3	2	1437	77 693	0.01	0
6-0600	0	440	0	3	1	1550	77 669	0.01	0
6-0630	0	207	0	3	1	1432	86 874	0.01	0
6-0700	0	224	0	3	1	1331	105 546	0.01	0
6-0730	0	595	0	3	2	1337	157 017	0.01	0
6-0800	0	210	0	3	1	1122	156 946	0.01	0
6-0830	0	249	0	3	1	1150	197 944	0.01	0
6-0900	0	195	0	3	1	1270	197 902	0.01	0
6-0930	0	386	0	3	2	1633	258 213	0.01	0
6-1000	0	246	0	3	1	1273	258 170	0.01	0
6-1030	0	190	0	3	2	1442	253 086	0.01	0
6-1100	0	233	0	3	1	1453	253 042	0.01	1
6-1130	0	275	0	3	2	1402	241 249	0.01	0
6-1200	0.02	86 449	0	3	1	1342	227 642	23.08	2
6-1230	0	44 077	0	3	1	1398	218 203	0.01	2
6-1300	0	259	0	1	1	1483	205 954	0.01	1
6-1330	0	19 486	0	3	0	1220	195 771	0.01	2
6-1400	0	16 866	0	3	1	1178	185 262	0.01	1
6-1430	0	50 117	0	3	1	1154	178 892	0.01	2
6-1500	0	322	0	2	1	970	191 119	0.01	1
6-1530	0	183	0	1	1	1284	214 085	0.01	0
6-1600	0	217	0	2	1	1051	252 878	0.01	0
6-1630	0	357	0	2	1	1372	273 263	0.01	2
6-1700	0	301	192	2	1	1288	296 734	0.01	0
6-1730	0	248	94	2	1	1140	310 027	0.01	1
6-1800	0	295	92	2	1	1133	336 449	0.01	1
6-1830	0	375	93	3	1	1120	350 309	0.01	0
6-1900	0	255	96	3	1	1086	369 687	0.01	0
6-1930	0	43 474	0	3	0	1232	374 882	19.10	75
6-2000	0	784	0	4	2	1446	382 243	0.01	1
6-2030	0	376	0	3	1	1202	392 216	0.01	0
6-2100	0	399	0	3	1	1406	407 688	0.01	0
6-2130	0	747	0	3	1	1659	420 342	0.01	0
6-2200	0.30	86 892	0	3	1	1232	438 840	0.01	2
6-2230	0	902	0	3	1	1621	447 262	0.01	0
6-2300	0.30	87 948	0	3	0	1384	459 839	0.01	1
6-2330	0	43 868	0	3	1	1526	462 713	32.42	53

Instance	Gap	Runtime	Slack	SS	SS+FD	Energy	Imbalance	Velo	Alg-Iter
7-0000	0	2578	18	2	1	1207	458 963	0.01	1
7-0030	0	264	18	2	1	1402	446 060	0.01	0
7-0100	0	276	17	2	0	1438	417 866	0.01	0
7-0130	0	255	115	2	1	1440	395 931	0.01	0
7-0200	0	265	41	2	1	1335	365 724	0.01	0
7-0230	0	234	47	2	1	1235	356 920	0.01	0
7-0300	0	259	56	2	0	1469	346 910	0.01	0
7-0330	0	233	67	2	1	1554	343 935	0.01	0
7-0400	0	262	84	2	1	1253	347 975	0.01	0
7-0430	0	256	89	2	1	1247	365 625	0.01	0
7-0500	0	267	98	2	1	1577	396 764	0.01	0
7-0530	0	350	91	2	1	1317	404 952	0.01	1
7-0600	0	201	0	2	0	1524	419 020	0.01	0
7-0630	0	206	0	2	1	1549	415 928	0.01	0
7-0700	0	249	106	2	1	1517	410 065	0.01	0
7-0730	0	241	132	2	1	1554	409 995	0.01	0
7-0800	0	228	106	2	1	1242	409 762	0.01	0
7-0830	0	242	111	2	1	1306	409 498	0.01	0
7-0900	0	221	117	2	1	1490	414 429	0.01	0
7-0930	0	253	114	2	1	1565	414 143	0.01	0
7-1000	0	238	110	2	1	1428	424 329	0.01	0
7-1030	0	457	109	2	1	1370	450 074	0.01	0
7-1100	0	610	15 164	2	1	1614	477 124	0.01	1
7-1130	0	3347	110	3	0	1402	486 046	0.01	2
7-1200	0	5223	114	3	1	1270	499 281	0.01	3
7-1230	0	2292	114	3	2	1447	493 248	0.01	3
7-1300	0	417	116	3	2	1385	479 548	0.01	1
7-1330	0	473	118	3	0	1423	476 858	0.01	2
7-1400	0	564	123	3	2	1233	455 319	0.01	2
7-1430	0	1891	126	3	2	1435	448 913	0.01	3
7-1500	0	358	0	2	1	1323	426 969	0.01	0
7-1530	0	342	0	2	1	1407	411 661	0.01	0
7-1600	0	421	0	2	1	1315	368 687	0.01	0
7-1630	0	251	0	2	1	1373	342 691	0.01	0
7-1700	0	202	0	2	1	1371	310 623	0.01	0
7-1730	0	206	0	2	1	1136	301 243	0.01	0
7-1800	0	180	0	2	1	1400	290 466	0.01	0
7-1830	0	196	0	2	0	1394	281 603	0.01	0
7-1900	0	197	0	2	1	1325	269 208	0.01	0
7-1930	0	202	0	2	1	1271	264 570	0.01	0
7-2000	0	188	0	2	1	1377	256 047	0.01	0
7-2030	0	184	0	2	1	1343	254 481	0.01	0
7-2100	0	179	0	2	1	1393	259 150	0.01	0
7-2130	0	235	0	2	1	1427	263 871	0.01	0
7-2200	0	193	0	2	0	1102	271 209	0.01	0
7-2230	0	176	0	2	1	1070	279 855	0.01	0
7-2300	0	190	0	2	1	1242	293 844	0.01	0
7-2330	0	188	0	2	1	1145	304 089	0.01	0

Instance	Gap	Runtime	Slack	SS	SS+FD	Energy	Imbalance	Velo	Alg-Iter
8-0000	0	193	0	2	0	974	314 633	0.01	0
8-0030	0	197	0	2	1	1131	321 220	0.01	0
8-0100	0	202	0	2	1	877	347 051	0.01	0
8-0130	0	179	0	2	1	1174	354 854	0.01	0
8-0200	0	179	0	2	1	858	357 759	0.01	0
8-0230	0	192	0	2	1	1197	367 979	0.01	0
8-0300	0	148	0	2	1	906	390 507	0.01	0
8-0330	0	175	0	2	1	909	396 681	0.01	0
8-0400	0	160	0	2	1	1044	394 515	0.01	0
8-0430	0	158	0	2	1	912	395 978	0.01	0
8-0500	0	191	0	2	1	990	402 989	0.01	0
8-0530	0	153	0	2	1	993	406 540	0.01	0
8-0600	0	160	0	2	1	999	415 207	0.01	0
8-0630	0	166	0	2	1	881	413 710	0.01	0
8-0700	0	178	0	2	1	1214	444 271	0.01	0
8-0730	0	188	0	2	1	924	459 459	0.01	0
8-0800	0	167	0	2	1	946	480 683	0.01	0
8-0830	0	181	0	2	1	1205	492 324	0.01	0
8-0900	0	190	0	2	1	1176	509 518	0.01	0
8-0930	0	280	0	2	1	778	527 872	0.01	0
8-1000	0	262	0	2	1	824	560 692	0.01	0
8-1030	0	5650	0	3	2	711	584 851	0.01	1
8-1100	0	1785	0	3	1	892	640 373	0.01	0
8-1130	0	3549	0	3	1	1000	700 407	0.01	0
8-1200	0.55	86 714	0	6	2	682	808 164	15.08	1
8-1230	0	92 531	0	4	2	962	885 048	0.01	0
8-1300	0.44	173 201	40 763	6	3	1208	989 728	18.66	1
8-1330	0.77	173 002	93 814	5	2	835	1 036 436	20.35	1
8-1400	0.80	173 186	145 952	4	3	875	1 105 801	17.35	1
8-1430	0.72	173 179	179 236	4	3	856	1 140 856	14.02	1
8-1500	0.59	172 927	220 459	5	2	814	1 180 952	13.99	1
8-1530	0.57	86 770	233 875	5	3	761	1 205 047	14.01	1
8-1600	0.61	173 472	351 372	5	2	851	1 243 176	0.01	0
8-1630	0.52	87 093	282 992	5	2	743	1 261 086	0.01	0
8-1700	0.51	87 119	302 612	5	1	759	1 273 903	0.01	0
8-1730	0.51	172 948	264 252	4	3	636	1 274 560	14.52	1
8-1800	0.49	173 367	283 546	4	2	741	1 274 986	0.01	0
8-1830	0.52	173 284	295 543	3	1	684	1 272 045	0.01	0
8-1900	0.48	86 551	246 966	3	1	630	1 267 022	15.14	1
8-1930	0.59	86 790	258 163	3	1	869	1 259 756	0.01	0
8-2000	0.65	86 486	220 385	3	2	988	1 252 633	36.99	1
8-2030	0.66	86 518	223 772	4	3	626	1 237 730	12.34	1
8-2100	0.74	86 669	185 860	4	2	534	1 210 868	12.80	1
8-2130	0.78	86 611	182 987	4	3	838	1 195 812	14.47	1
8-2200	0.82	86 729	402 012	5	2	526	1 179 157	0.01	0
8-2230	0.74	86 541	143 437	4	3	554	1 157 811	11.96	1
8-2300	0.73	86 719	144 282	4	1	775	1 117 023	0.01	0
8-2330	0.74	86 481	98 534	4	3	930	1 094 006	25.83	1

Instance	Gap	Runtime	Slack	SS	SS+FD	Energy	Imbalance	Velo	Alg-Iter
9-0000	0.70	86 490	112 019	4	2	721	1 065 932	18.30	1
9-0030	0.63	86 876	111 612	4	1	761	1 057 529	0.01	0
9-0100	0.55	86 642	50 260	4	1	748	1 038 288	13.63	1
9-0130	0.48	86 503	42 128	4	2	697	1 027 563	19.09	1
9-0200	0.18	122 705	85 091	4	2	688	1 014 642	0.01	1
9-0230	0	52 016	39 484	4	2	725	996 413	0.01	2
9-0300	0	2944	12 943	3	1	728	966 323	0.01	1
9-0330	0	3049	1168	3	2	675	948 605	0.01	0
9-0400	0	7851	1735	3	2	675	924 325	0.01	2
9-0430	0	6106	1926	3	2	610	906 729	0.01	1
9-0500	0	2996	3144	3	3	613	879 644	0.01	0
9-0530	0	1096	2504	3	3	585	863 484	0.01	0
9-0600	0	4248	1166	2	0	618	838 026	0.01	0
9-0630	0	2973	1530	2	2	625	815 211	0.01	1
9-0700	0	530	12 031	1	1	710	784 628	0.01	1
9-0730	0	376	2075	2	1	691	759 199	0.01	0
9-0800	0	446	919	2	1	625	722 542	0.01	0
9-0830	0	247	1110	2	2	593	698 156	0.01	0
9-0900	0	244	1600	2	1	585	662 707	0.01	0
9-0930	0	297	1590	2	1	566	634 654	0.01	0
9-1000	0	280	644	1	1	571	587 544	0.01	0

Results for test set H2-EQ

The columns of the following tables contain the results of the computational experiments for test set H2-EQ described and discussed in Section 4. Here, the first column contains the instance name. It consists of the virtual day together with the time in hours and minutes of the corresponding initial state, i.e., 2-0400 is the instance having the initial state from 4am of virtual day 2. The second column denotes the optimality gap for the last solve of a MILP during the tri-level MILP model solve. The third column states the run time of the complete algorithmic approach Algorithm 2 for the corresponding instance until it was terminated. In the fourth column, the total absolute slack used in this instance in kg is given. While the fifth column denotes the total number of conducted simple state changes, the sixth column accounts only for those in which a flow direction change was performed simultaneously. Next, the seventh column states the amount of compression energy that was used in MWh. Finally, while the eighth column denotes the flow imbalance in kg, the last column states the number of iterations of Algorithm 2, which is equivalent to the number of added no-good-cuts.

Instance	Gap	Runtime	Slack	SS	SS+FD	Energy	Imbalance	Velo	Alg-Iter
1-1200	0	6346	0	3	2	2181	430 746	0.01	0
1-1230	0	6176	0	2	2	2185	440 000	0.01	0
1-1300	0	4288	0	3	2	2108	478 177	0.01	0
1-1330	0	3496	0	3	2	2224	523 839	0.01	0
1-1400	0	9856	0	4	2	2054	546 922	0.01	0
1-1430	0	14 254	0	4	3	1883	551 993	0.01	0
1-1500	0	14 021	0	3	2	1847	576 418	0.01	0
1-1530	0.06	86 595	0	4	3	1766	582 213	0.01	0
1-1600	0	32 846	0	4	2	1804	595 714	0.01	0
1-1630	0.14	86 557	0	4	2	1733	594 914	0.01	0
1-1700	0	14 122	0	4	2	1778	567 160	0.01	0
1-1730	0	21 216	0	4	3	1758	553 627	0.01	0
1-1800	0	31 516	0	4	2	1799	525 065	0.01	0
1-1830	0	11 727	0	4	2	1796	514 221	0.01	0
1-1900	0	2245	0	3	2	1924	482 288	0.01	0
1-1930	0	2910	0	3	2	1952	466 172	0.01	0
1-2000	0	195	1295	3	2	1882	418 967	0.01	0
1-2030	0	271	0	3	2	1839	393 754	0.01	0
1-2100	0	629	0	3	2	1820	344 425	0.01	0
1-2130	0	313	0	3	2	1838	325 500	0.01	0
1-2200	0	384	2382	3	2	1896	279 837	0.01	0
1-2230	0	2217	0	3	2	1928	264 773	0.01	0
1-2300	0	2738	0	3	2	1794	221 356	0.01	0
1-2330	0	2062	0	3	2	1832	208 580	0.01	0

Instance	Gap	Runtime	Slack	SS	SS+FD	Energy	Imbalance	Velo	Alg-Iter
2-0000	0	267	34 659	2	1	1810	194 599	0.01	0
2-0030	0	148	0	2	1	1842	184 692	0.01	0
2-0100	0	155	0	2	1	1852	156 098	0.01	0
2-0130	0	152	0	2	1	1835	145 868	0.01	0
2-0200	0	277	9815	2	1	1875	135 902	0.01	0
2-0230	0	215	0	3	2	1833	134 278	0.01	0
2-0300	0	180	0	3	2	1708	106 841	0.01	0
2-0330	0	178	0	3	2	1983	92 562	0.01	0
2-0400	0	758	16 596	2	1	1853	71 698	0.01	0
2-0430	0	213	0	3	2	1840	60 980	0.01	0
2-0500	0	171	0	3	2	1636	25 726	0.01	0
2-0530	0	188	0	3	2	1646	16 725	0.01	0
2-0600	0	196	14 120	2	1	1614	14 604	0.01	0
2-0630	0	177	0	3	2	1639	16 306	0.01	0
2-0700	0	189	0	3	2	1607	46 642	0.01	0
2-0730	0	179	0	3	2	1778	62 201	0.01	0
2-0800	0	378	2096	3	2	1685	90 478	0.01	0
2-0830	0	190	0	3	2	1648	109 903	0.01	0
2-0900	0	336	0	3	2	1679	138 494	0.01	0
2-0930	0	175	0	3	2	1608	150 667	0.01	0
2-1000	0	364	1220	3	2	1563	181 105	0.01	0
2-1030	0	183	0	3	2	1904	182 113	0.01	0
2-1100	0	196	0	3	2	1662	202 106	0.01	0
2-1130	0	187	0	3	2	1878	202 845	0.01	0
2-1200	0	514	929	3	2	1793	212 077	0.01	0
2-1230	0	190	0	3	2	1706	212 022	0.01	0
2-1300	0	199	0	3	2	1928	242 573	0.01	0
2-1330	0	250	0	3	2	1606	245 712	0.01	0
2-1400	0	366	0	5	4	1489	274 828	0.01	0
2-1430	0	212	0	3	2	1887	281 016	0.01	0
2-1500	0	515	242	3	2	1570	299 028	0.01	0
2-1530	0	344	0	3	2	1607	295 588	0.01	0
2-1600	0	420	2033	3	2	1664	296 326	0.01	0
2-1630	0	232	0	3	2	1490	302 506	0.01	0
2-1700	0	199	0	3	2	1415	311 970	0.01	0
2-1730	0	242	0	3	2	1669	306 921	0.01	0
2-1800	0	692	1812	3	2	1435	210 848	0.01	0
2-1830	0	193	0	3	2	1353	175 202	0.01	0
2-1900	0	915	1670	3	2	1365	133 193	0.01	0
2-1930	0	212	0	3	2	1342	116 817	0.01	0
2-2000	0	208	0	3	2	1395	86 308	0.01	0
2-2030	0	175	0	3	2	1349	67 988	0.01	0
2-2100	0	3153	0	3	2	1320	20 281	0.01	0
2-2130	0	203	0	3	2	1162	−423	0.01	0
2-2200	0	254	0	3	1	1281	−49 453	0.01	0
2-2230	0	214	0	3	2	1248	−72 196	0.01	0
2-2300	0	883	0	3	2	1188	−142 092	0.01	0
2-2330	0	192	0	3	2	1198	−160 639	0.01	0

Instance	Gap	Runtime	Slack	SS	SS+FD	Energy	Imbalance	Velo	Alg-Iter
3-0000	0	207	0	3	2	1123	−195 442	0.01	0
3-0030	0	213	0	3	2	1276	−202 299	0.01	0
3-0100	0	211	0	3	2	1250	−226 317	0.01	0
3-0130	0	195	0	3	2	1193	−236 757	0.01	0
3-0200	0	555	854	3	2	1100	−253 760	0.01	0
3-0230	0	213	25 982	3	2	1156	−256 897	0.01	0
3-0300	0	198	0	3	1	1165	−265 458	0.01	0
3-0330	0	240	0	3	2	1328	−270 428	0.01	0
3-0400	0	236	950	3	2	1179	−279 786	0.01	0
3-0430	0	248	24 893	3	2	1481	−287 263	0.01	0
3-0500	0	726	16 800	3	1	1048	−313 340	0.01	0
3-0530	0	523	22 976	3	2	1339	−323 575	0.01	0
3-0600	0	215	758	3	1	1252	−348 097	0.01	0
3-0630	0	392	116 195	3	2	1253	−356 786	0.01	0
3-0700	0	226	154 812	3	2	1363	−409 850	0.01	0
3-0730	0	458	158 748	3	2	1310	−437 793	0.01	0
3-0800	0	767	267 699	3	2	1176	−478 135	0.01	0
3-0830	0	773	267 699	3	2	1176	−478 135	0.01	0
3-0900	0	302	149 684	2	2	1122	−518 436	0.01	0
3-0930	0	447	152 616	2	2	1198	−516 675	0.01	0
3-1000	0	200	257 345	2	2	1224	−432 387	0.01	0
3-1030	0	399	226 129	2	2	1524	−374 209	0.01	0
3-1100	0	153	144 879	1	1	1336	−310 693	0.01	0
3-1130	0	180	147 967	1	1	1085	−263 924	0.01	0
3-1200	0	308	280 272	1	1	1252	−183 002	0.01	0
3-1230	0	985	238 629	1	1	1210	−121 134	0.01	0
3-1300	0	227	144 672	1	1	1167	−46 096	0.01	0
3-1330	0	243	79 953	1	1	1264	−822	0.01	0
3-1400	0	324	210 849	1	1	1398	51 158	0.01	0
3-1430	0	152	123 070	1	1	1344	90 007	0.01	0
3-1500	0	170	40 794	1	1	1384	146 712	0.01	0
3-1530	0	193	86 333	1	1	1344	170 208	0.01	0
3-1600	0	278	157 897	2	2	1439	207 018	0.01	0
3-1630	0	193	111 332	1	1	1276	223 484	0.01	0
3-1700	0	148	34 512	1	1	1118	256 950	0.01	0
3-1730	0	195	25 156	1	1	1223	280 019	0.01	0
3-1800	0	300	139 233	2	2	1153	337 865	0.01	0
3-1830	0	655	67 788	2	2	1079	371 431	0.01	0
3-1900	0	241	26 173	1	1	1188	411 331	0.01	0
3-1930	0	488	37 649	2	2	1111	429 550	0.01	0
3-2000	0	1715	153 376	3	2	889	450 524	0.01	0
3-2030	0	613	64 332	2	2	1374	467 205	0.01	0
3-2100	0	170	1497	2	1	1263	502 260	0.01	0
3-2130	0	164	1320	2	2	1255	513 603	0.01	0
3-2200	0	4126	117 176	3	2	1011	545 099	0.01	0
3-2230	0	204	22 678	2	1	1265	563 512	0.01	0
3-2300	0	365	840	2	1	1219	598 425	0.01	0
3-2330	0	4379	18 556	2	1	1268	607 776	0.01	0

Instance	Gap	Runtime	Slack	SS	SS+FD	Energy	Imbalance	Velo	Alg-Iter
4-0000	0	13 969	107 958	4	2	979	632 892	0.01	0
4-0030	0	9497	34 871	2	2	995	620 643	0.01	0
4-0100	0	253	7319	2	2	1144	606 254	0.01	0
4-0130	0	182	2941	2	2	1117	588 549	0.01	0
4-0200	0	1455	81 729	3	2	964	559 805	0.01	0
4-0230	0	645	8768	2	2	1131	533 122	0.01	1
4-0300	0	634	3636	2	2	1100	508 809	0.01	0
4-0330	0	177	4940	2	1	1091	492 173	0.01	0
4-0400	0	835	61 071	2	2	862	472 938	0.01	0
4-0430	0	464	4442	2	1	1038	456 948	0.01	0
4-0500	0	376	4788	2	1	1061	432 797	0.01	0
4-0530	0	175	5449	2	1	1020	398 782	0.01	0
4-0600	0	221	4781	2	1	1026	348 879	0.01	0
4-0630	0	187	4504	1	1	958	338 132	0.01	0
4-0700	0	175	5124	1	1	970	374 623	0.01	0
4-0730	0	180	5978	1	1	1003	372 955	0.01	0
4-0800	0	419	5613	1	1	1013	358 462	0.01	0
4-0830	0	451	5537	1	1	1041	315 626	0.01	0
4-0900	0	275	5143	1	1	985	208 331	0.01	0
4-0930	0	176	5992	1	1	1018	117 422	0.01	0
4-1000	0	224	5911	1	1	1211	−40 503	0.01	0
4-1030	0	256	6245	1	1	1043	−128 564	0.01	0
4-1100	0	218	5110	1	1	1249	−238 887	0.01	0
4-1130	0	308	5585	1	1	1499	−312 900	0.01	0
4-1200	0	241	5989	1	1	1546	−433 837	0.01	0
4-1230	0	240	11 703	1	1	1623	−524 401	0.01	0
4-1300	0	296	49 758	1	1	1382	−628 128	0.01	1
4-1330	0	354	24 172	2	1	1567	−687 185	0.01	1
4-1400	0	1311	9171	2	1	1582	−748 982	0.01	1
4-1430	0	783	10 565	2	1	1634	−786 476	0.01	1
4-1500	0	1396	9797	2	2	1889	−841 777	0.01	2
4-1530	0	6016	77 086	3	2	3077	−859 548	0.01	3
4-1600	0	1062	29 405	2	2	1857	−887 949	0.01	2
4-1630	0	3810	8218	2	2	2042	−905 390	0.01	2
4-1700	0	1301	61 172	2	2	1991	−959 253	0.01	2
4-1730	0	4318	63 216	5	3	3772	−1 006 823	0.01	2
4-1800	0	1315	8020	3	2	2444	−1 052 770	0.01	2
4-1830	0	1868	10 632	3	1	2432	−1 071 994	0.01	2
4-1900	0	841	6339	3	1	3187	−1 093 270	0.01	2
4-1930	0	4477	91 373	5	4	3647	−1 101 170	0.01	2
4-2000	0	2051	7261	3	2	3370	−1 110 754	0.01	2
4-2030	0	1656	8412	3	1	4125	−1 118 477	0.01	2
4-2100	0	2517	6330	3	1	3743	−1 116 831	0.01	2
4-2130	0	4775	91 757	5	4	4257	−1 104 664	0.01	2
4-2200	0	7667	87 713	5	3	3488	−1 095 882	0.01	3
4-2230	0	1932	8213	3	2	4887	−1 080 405	0.01	2
4-2300	0	3612	47 913	4	2	4391	−1 064 272	0.01	2
4-2330	0	6626	66 193	5	3	4510	−1 045 333	0.01	2

Instance	Gap	Runtime	Slack	SS	SS+FD	Energy	Imbalance	Velo	Alg-Iter
6-0000	0	192	0	3	1	2249	−171 890	0.01	0
6-0030	0	398	0	3	1	2126	−128 339	0.01	0
6-0100	0	294	0	3	1	2184	−128 397	0.01	0
6-0130	0	677	0	3	1	2187	−87 263	0.01	0
6-0200	0	1648	0	3	1	1986	−87 304	0.01	0
6-0230	0	197	0	3	2	2169	−872	0.01	0
6-0300	0	214	0	3	2	1945	−872	0.01	0
6-0330	0	482	0	3	2	2118	66 309	0.01	0
6-0400	0	226	0	3	1	2338	66 306	0.01	0
6-0430	0	235	0	3	1	2364	71 892	0.01	0
6-0500	0	299	0	3	2	2163	71 907	0.01	0
6-0530	0	227	0	3	1	2295	109 523	0.01	0
6-0600	0	211	0	3	2	2423	109 491	0.01	0
6-0630	0	232	0	3	2	2082	126 457	0.01	0
6-0700	0	222	0	3	1	2204	151 353	0.01	0
6-0730	0	560	0	3	1	2125	220 415	0.01	0
6-0800	0	719	0	3	2	2304	220 321	0.01	0
6-0830	0.30	86 590	0	4	1	2137	275 549	0.01	0
6-0900	0.28	86 606	0	4	3	1892	275 492	0.01	0
6-0930	0.43	86 586	0	4	1	1901	356 913	0.01	0
6-1000	0.23	86 680	0	4	3	2087	356 856	0.01	0
6-1030	0	32 836	0	4	2	1952	348 194	0.01	0
6-1100	0	46 675	0	4	1	1775	348 135	0.01	0
6-1130	0.32	86 615	0	4	1	1841	333 067	0.01	0
6-1200	0.28	86 650	0	4	2	1893	316 244	0.01	0
6-1230	0.25	89 900	0	4	1	1764	304 191	31.15	2
6-1300	0	48 500	0	3	1	1683	288 404	30.97	2
6-1330	0.26	101 880	0	4	0	1977	276 664	0.01	2
6-1400	0	82 871	0	4	1	2327	267 046	0.01	1
6-1430	0	93 561	0	4	2	1808	261 410	0.01	1
6-1500	0	4465	0	3	1	2055	276 359	0.01	2
6-1530	0	346	0	1	1	2048	301 544	0.01	0
6-1600	0	100 276	0	4	2	1926	344 433	0.01	1
6-1630	0	66 301	0	4	1	2286	365 321	0.01	0
6-1700	0	4639	26 019	3	1	2041	388 697	0.01	0
6-1730	0	954	14 106	3	2	2015	401 686	0.01	0
6-1800	0	24 246	729	3	1	1999	429 839	0.01	0
6-1830	0	39 196	26 365	5	2	2101	446 814	0.01	0
6-1900	0	9258	25 891	4	1	1980	471 127	0.01	0
6-1930	0	47 247	2436	5	1	2072	479 559	0.01	1
6-2000	0.17	86 469	609	5	0	2370	492 256	30.09	1
6-2030	0	70 807	684	4	2	1971	505 387	0.01	0
6-2100	0.22	86 575	25 949	4	1	1865	525 958	0.01	0
6-2130	0.01	86 517	632	6	3	2006	541 404	31.30	1
6-2200	0.26	86 531	34 044	6	3	2045	563 204	31.25	1
6-2230	0.27	86 645	25 947	5	1	2169	573 947	0.01	0
6-2300	0.37	86 617	661	7	4	2004	590 517	0.01	0
6-2330	0.31	86 658	719	6	4	2117	594 826	0.01	0

Instance	Gap	Runtime	Slack	SS	SS+FD	Energy	Imbalance	Velo	Alg-Iter
7-0000	0.54	86 647	660	6	4	2039	590 719	0.01	0
7-0030	0	36 122	716	4	1	2438	574 837	0.01	0
7-0100	0	5746	698	3	1	1986	539 009	0.01	0
7-0130	0	6238	704	3	1	1833	509 623	0.01	0
7-0200	0	51 541	749	3	0	1945	469 391	0.01	0
7-0230	0	2342	737	4	1	2498	459 580	0.01	0
7-0300	0	1636	712	3	0	2070	449 586	0.01	0
7-0330	0	1080	766	3	1	2011	447 737	0.01	0
7-0400	0	1228	783	3	0	2148	455 986	0.01	0
7-0430	0	4623	776	3	0	2133	480 075	0.01	0
7-0500	0	15 791	788	3	1	1978	522 168	0.01	0
7-0530	0	11 280	804	3	1	1978	533 792	0.01	0
7-0600	0	2915	7238	3	1	2023	553 524	0.01	2
7-0630	0	7030	11 554	3	1	1962	549 987	0.01	2
7-0700	0	40 475	792	3	0	2334	543 925	0.01	0
7-0730	0	54 374	785	5	3	2110	544 812	0.01	0
7-0800	0	11 403	786	3	1	1977	545 398	0.01	0
7-0830	0	7619	790	5	2	2095	545 835	0.01	0
7-0900	0	1937	757	4	2	1997	553 186	0.01	1
7-0930	0	802	759	4	2	2145	555 222	0.01	0
7-1000	0	1323	756	4	1	1969	571 546	0.01	0
7-1030	0	4881	764	4	2	1980	604 717	0.01	0
7-1100	0	63 169	20 843	5	2	2457	638 114	0.01	1
7-1130	0.42	86 686	787	4	2	1912	647 610	0.01	0
7-1200	0.10	86 422	759	4	2	2100	662 012	28.25	1
7-1230	0.13	86 632	717	4	2	1959	652 085	0.01	0
7-1300	0.05	86 462	20 823	5	2	2319	630 653	31.72	1
7-1330	0.28	114 693	700	4	0	2068	625 193	0.01	1
7-1400	0.02	86 500	7604	4	3	1854	594 080	28.86	1
7-1430	0.23	100 103	790	4	1	1929	583 940	0.01	2
7-1500	0	16 866	812	4	2	1817	552 425	0.01	3
7-1530	0	5024	14 528	4	2	2040	530 531	0.01	2
7-1600	0	2428	20 017	4	2	2006	471 432	0.01	1
7-1630	0	14 464	8757	4	2	1997	435 277	0.01	1
7-1700	0	10 179	9004	4	2	1894	390 318	0.01	1
7-1730	0	1347	641	4	2	1927	376 910	0.01	0
7-1800	0	4351	7724	4	2	2019	362 033	0.01	0
7-1830	0	1500	418	4	2	1892	351 114	0.01	0
7-1900	0	367	16 741	3	2	2011	336 246	0.01	0
7-1930	0	362	394	3	1	2044	331 369	0.01	0
7-2000	0	826	7258	3	1	1965	322 116	0.01	0
7-2030	0	352	170	3	1	1924	321 053	0.01	0
7-2100	0	442	171	3	0	1934	329 127	0.01	0
7-2130	0	1654	170	3	1	1965	336 639	0.01	0
7-2200	0	7838	7076	3	2	1920	347 719	0.01	2
7-2230	0	18 826	0	3	2	1881	360 541	0.01	0
7-2300	0	212	0	2	1	1819	381 590	0.01	0
7-2330	0	37 386	0	3	2	1824	397 058	0.01	0

Instance	Gap	Runtime	Slack	SS	SS+FD	Energy	Imbalance	Velo	Alg-Iter
8-0000	0	15 602	0	3	1	1923	412 500	0.01	0
8-0030	0	24 505	0	3	2	1894	420 407	0.01	0
8-0100	0	32 839	0	3	2	1716	452 389	0.01	0
8-0130	0	20 243	0	3	2	1780	460 506	0.01	0
8-0200	0	42 032	0	3	2	1631	460 823	0.01	0
8-0230	0	24 550	0	3	1	1595	473 796	0.01	0
8-0300	0	8284	0	3	2	1638	503 395	0.01	0
8-0330	0	28 990	0	3	2	1560	511 735	0.01	0
8-0400	0	7643	0	3	2	1564	509 799	0.01	0
8-0430	0	830	0	2	1	1779	513 536	0.01	0
8-0500	0	1107	0	2	1	1804	526 432	0.01	0
8-0530	0	30 756	0	3	1	1359	532 579	0.01	0
8-0600	0	6250	0	3	2	1603	547 076	0.01	0
8-0630	0	1048	0	3	1	1424	545 037	0.01	0
8-0700	0	66 715	0	4	2	1224	585 860	0.01	0
8-0730	0	65 265	0	4	1	1498	606 647	0.01	0
8-0800	0	67 326	0	3	1	1451	635 931	0.01	0
8-0830	0	82 469	0	4	3	1118	651 996	0.01	0
8-0900	0.25	86 605	0	4	2	1574	676 269	0.01	0
8-0930	0	70 576	0	4	2	1131	701 304	0.01	0
8-1000	0.50	86 697	0	5	2	1205	747 797	0.01	0
8-1030	0.62	86 791	0	7	1	1297	782 849	0.01	0
8-1100	0.60	173 372	62 787	5	3	1969	859 354	0.01	0
8-1130	0.72	173 187	157 279	5	3	1885	939 609	0.01	0
8-1200	0.48	173 064	258 215	5	2	2330	1 084 682	0.01	0
8-1230	0.38	87 130	444 418	5	2	2073	1 186 122	0.01	0
8-1300	0.28	130 799	491 660	5	1	2358	1 323 768	0.01	0
8-1330	0.27	120 370	602 235	4	0	2127	1 385 263	0.01	0
8-1400	0.23	86 828	678 511	4	2	2356	1 475 302	0.01	0
8-1430	0.19	86 896	782 431	4	1	2620	1 521 135	0.01	0
8-1500	0.19	87 333	979 930	5	2	2537	1 571 669	0.01	0
8-1530	0.20	95 932	805 310	5	2	2494	1 601 548	0.01	0
8-1600	0.19	99 618	836 074	5	3	2362	1 646 850	0.01	0
8-1630	0.19	86 737	767 605	5	2	1494	1 666 840	21.49	1
8-1700	0.20	87 295	792 990	5	2	997	1 678 358	0.01	0
8-1730	0.19	99 122	762 181	5	2	1000	1 677 617	0.01	0
8-1800	0.19	119 252	794 079	5	2	933	1 677 008	0.01	0
8-1830	0.19	86 642	772 338	5	3	926	1 672 400	0.01	0
8-1900	0.17	86 652	750 866	5	1	891	1 664 337	0.01	0
8-1930	0.18	86 695	763 190	5	3	855	1 654 413	0.01	0
8-2000	0.19	86 690	769 698	5	2	884	1 644 743	0.01	0
8-2030	0.19	86 668	715 252	5	2	903	1 624 589	0.01	0
8-2100	0.20	86 634	730 350	5	2	858	1 588 731	0.01	0
8-2130	0.21	86 636	679 414	5	3	865	1 569 048	0.01	0
8-2200	0.22	86 630	631 910	5	2	998	1 547 703	0.01	0
8-2230	0.22	86 622	654 304	5	1	909	1 520 112	0.01	0
8-2300	0.23	86 545	583 351	5	2	1082	1 466 850	17.83	1
8-2330	0.24	86 657	586 134	5	1	967	1 437 082	0.01	0

Instance	Gap	Runtime	Slack	SS	SS+FD	Energy	Imbalance	Velo	Alg-Iter
9-0000	0.24	86 611	575 751	5	1	812	1 399 948	0.01	0
9-0030	0.25	86 605	540 665	5	1	885	1 387 964	0.01	0
9-0100	0.27	86 596	513 071	5	2	863	1 361 985	0.01	0
9-0130	0.28	86 627	474 020	5	1	871	1 345 399	0.01	0
9-0200	0.26	86 598	435 578	5	2	928	1 323 635	0.01	0
9-0230	0.34	86 613	425 831	5	3	908	1 297 955	0.01	0
9-0300	0.33	86 594	365 500	5	2	959	1 256 854	0.01	0
9-0330	0.33	86 598	378 808	5	2	1026	1 231 430	0.01	0
9-0400	0.43	86 633	423 940	6	2	870	1 195 135	0.01	0
9-0430	0.41	86 587	287 528	6	2	1033	1 169 756	0.01	0
9-0500	0.33	86 584	327 926	6	2	958	1 131 561	0.01	0
9-0530	0.45	86 575	434 297	5	3	865	1 107 515	0.01	0
9-0600	0.63	86 586	165 577	4	2	904	1 070 134	0.01	0
9-0630	0.63	86 578	212 081	4	1	943	1 037 251	0.01	0
9-0700	0.55	86 635	97 814	4	1	916	993 232	0.01	0
9-0730	0.43	86 574	66 168	5	2	894	957 915	0.01	0
9-0800	0	4525	3678	4	2	834	906 490	0.01	0
9-0830	0	2337	5118	3	2	793	872 017	0.01	1
9-0900	0	966	4142	3	2	826	822 156	0.01	0
9-0930	0	1762	4414	3	2	726	784 112	0.01	1
9-1000	0	1052	3997	3	1	671	720 878	0.01	0